

PAPER

G2DR: A Genotype-First Framework for Genetics-Informed Target Prioritization and Drug Repurposing

Muhammad Muneeb^{1,2} and David B. Ascher^{1,2,*}

¹School of Chemistry and Molecular Biology, The University of Queensland, Queen Street, 4067, Queensland, Australia and

²Computational Biology and Clinical Informatics, Baker Heart and Diabetes Institute, Commercial Road, 3004, Victoria, Australia

*Corresponding author: David B. Ascher, Email: d.ascher@uq.edu.au

Abstract

Human genetics offers a promising route to therapeutic discovery, yet practical frameworks that translate genotype-derived signal into ranked target and drug hypotheses remain limited, particularly when matched disease transcriptomics are unavailable. Here, we present G2DR, a genotype-first computational prioritization framework that propagates inherited genetic variation through genetically predicted gene expression, multi-method gene-level testing, pathway enrichment, network context, druggability, and multi-source drug–target evidence integration to generate ranked hypotheses for downstream follow-up. In a migraine case study using 733 UK Biobank participants (53 cases and 680 controls) under stratified five-fold cross-validation, we imputed genetically regulated expression across seven transcriptome-weight resources and ranked genes using a reproducibility-aware discovery score derived exclusively from training and validation data, followed by a balanced integrated score for downstream target selection. In held-out evaluation, discovery-based prioritization generalized to unseen data, achieving a gene-level ROC-AUC of 0.775 and PR-AUC of 0.475 for recovery of test-significant genes, while retaining enrichment for curated migraine-associated biology. Mapping prioritized genes to compounds through Open Targets, DGIdb, and ChEMBL yielded candidate drug sets enriched for migraine-linked and literature-associated compounds relative to a global drug background, although recovery was strongest for broader mechanism-linked and off-label therapeutic space rather than migraine-specific approved therapies. Directionality filtering further separated broadly recovered compounds from those with stronger mechanistic compatibility. G2DR should therefore be interpreted as a modular computational prioritization framework for genetics-informed hypothesis generation and follow-up in genotype-first settings, not as a clinically actionable target-identification or drug-recommendation system. All prioritized genes and compounds require independent experimental, pharmacological, and clinical validation. Supplementary data are available at *Briefings in Bioinformatics* online.

Key words: drug repurposing, human genetics, TWAS, genetically predicted expression, target prioritization, translational bioinformatics

Introduction

Drug repurposing remains an attractive strategy for accelerating therapeutic development because existing compounds benefit from prior pharmacological, toxicological, and manufacturing knowledge ([1, 2, 3]). Over the past two decades, computational repurposing has expanded from expression-signature matching ([4]) and network medicine ([5, 6, 7]) to machine-learning and knowledge-graph approaches that integrate heterogeneous biomedical evidence at scale ([8, 9]). Yet many current pipelines depend on disease-specific transcriptomic profiles ([10, 11]), curated disease modules ([6, 12]), or historical drug–disease labels ([2, 8]), which can be limiting for newly studied phenotypes or for biobank settings where genotype and phenotype labels are available but disease-relevant molecular profiling is sparse or absent ([13, 14, 2, 15]).

Human genetics provides a particularly attractive starting point for therapeutic prioritization because inherited variation is stable, scalable, and increasingly well characterized across large cohorts ([13, 14]). When measured expression is unavailable, genotype can be propagated through transcriptome imputation models to estimate genetically regulated expression ([16, 17]), offering an interpretable intermediate layer between variant-level signal and candidate genes ([15]). This strategy is appealing, but it also comes with important caveats: TWAS-style approaches prioritize genes associated with trait-linked regulatory signal, not necessarily causal effector genes ([15]), and inference remains sensitive to linkage disequilibrium, co-regulation, tissue context, ancestry, and model architecture ([15, 18]). These limitations argue for integrative frameworks that improve robustness and interpretability rather than relying

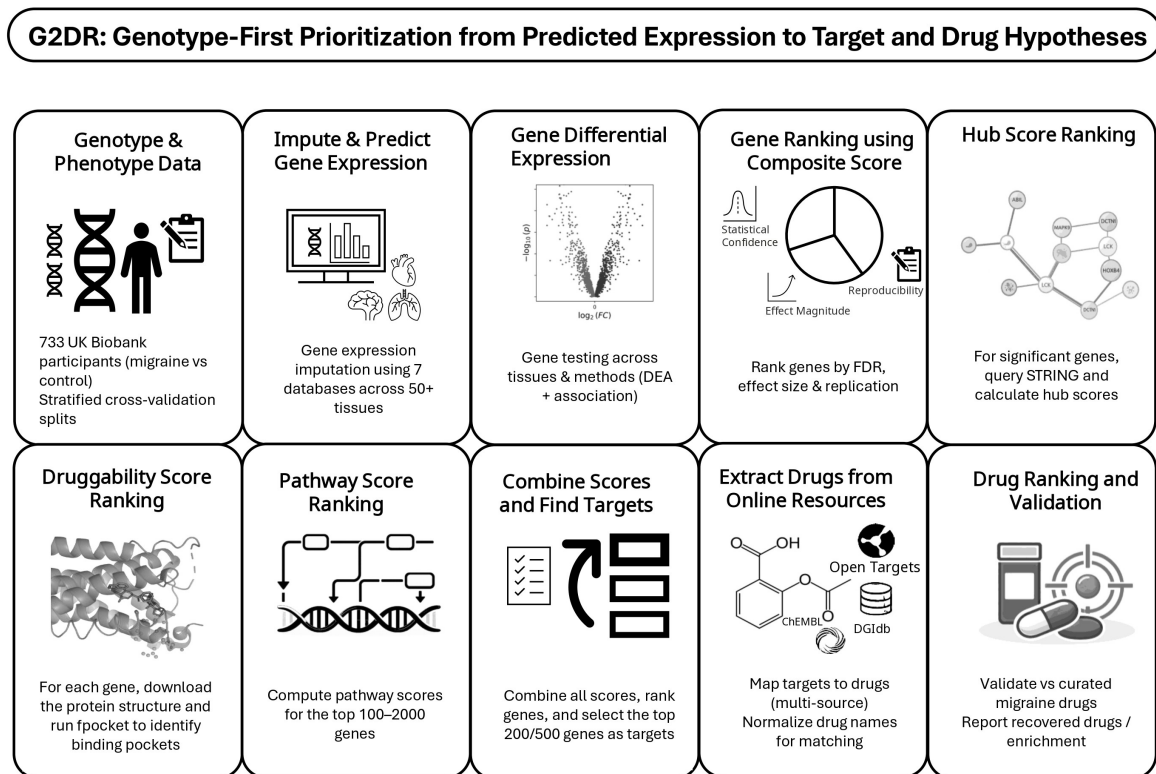


Fig. 1. Overview of the G2DR framework. Genotype and phenotype data from the migraine cohort were partitioned by stratified cross-validation and propagated through genotype-based transcriptome imputation across multiple expression-weight resources. Covariate-adjusted predicted expression values were tested using multiple differential-expression and association methods, and significant results from the training and validation splits were aggregated into a discovery set. Genes were then ranked using a composite score that integrated reproducibility, effect magnitude, and statistical confidence, followed by pathway, network, and druggability annotation to generate an integrated target-prioritization score. Top-ranked genes were mapped to candidate compounds through Open Targets, DGIdb, and ChEMBL, and the resulting drug lists were evaluated against curated migraine-associated drug references.

on any single transcriptome-prediction resource or analytical test ([15]).

A further motivation comes from therapeutic translation. Multiple studies have shown that targets supported by human genetics are more likely to succeed in clinical development ([19, 20]), making genetics-informed target selection an increasingly important component of drug discovery. However, the key translational challenge is not simply to detect associated genes, but to prioritize those with the strongest convergent support and then connect them to tractable pharmacological hypotheses in a transparent and reproducible manner.

Here, we present G2DR (Figure 1), a genotype-first computational framework for genetics-informed target prioritization and drug repurposing hypothesis generation. G2DR integrates genetically predicted expression (Table 1) from multiple transcriptome-weight resources ([16, 17, 15]), multi-method gene-level testing, pathway enrichment, network context, structure- and knowledge-based druggability, and multi-source drug–target evidence ([21, 22, 23, 24, 25]) to generate ranked computational hypotheses for candidate targets and associated compounds, without requiring measured disease transcriptomics or supervised training on curated indication labels ([2]).

We demonstrate the framework in migraine using UK Biobank data and evaluate performance at multiple levels, including held-out gene replication, enrichment for curated

migraine biology, and recovery of migraine-linked drugs from prioritized targets. Framed explicitly as a computational prioritization engine for downstream experimental follow-up rather than a clinically actionable target-identification system, G2DR is best viewed as a modular proof-of-concept framework with clear room for further maturation.

Methods

Study Design and Cohort Assembly

A total of 733 participants (53 cases and 680 controls) who reported migraine and recorded comorbid conditions, including hypertension, asthma, depression, osteoarthritis, hypercholesterolemia, irritable bowel syndrome, hypothyroidism, hay fever, and gastroesophageal reflux disease, were extracted from the UK Biobank ([13, 14]). These comorbidities are commonly reported to co-occur with migraine ([31, 32, 33, 34]). Genotype–phenotype data were partitioned using stratified five-fold cross-validation, with each fold split into training (80%), validation (10%), and test (10%) subsets to preserve the case–control ratio. Genotype quality control was applied within each training fold and propagated to validation and test subsets, including per-variant filters for minor allele frequency (MAF) ≥ 0.01 , Hardy–Weinberg equilibrium (HWE) $p \geq 1 \times 10^{-6}$, and variant missingness ≤ 0.1 , along with per-individual

Table 1. Expression weight models used for genotype-based gene expression prediction.

| Model | Source | Description | Gene-Tissue Pairs | |
|---------|---|---|-------------------|------|
| MASHR | https://zenodo.org/records/7551845 | Multivariate adaptive shrinkage models for cross-population transcriptome prediction, designed to improve TWAS performance in underrepresented populations [26] | 686,241 (tissues) | (49) |
| JTI | https://zenodo.org/records/3842289 | Joint-tissue imputation models that borrow information across tissues via shared genetic regulation, enabling both expression prediction and downstream causal inference [27] | 533,141 (tissues) | (49) |
| CTIMP | https://github.com/yiminghu/CTIMP | Cross-tissue gene-expression imputation models trained with sparse group-LASSO to borrow information across GTEx tissues [28] | 404,450 (tissues) | (49) |
| UTMOST | https://zenodo.org/records/3842289 | Cross-tissue transcriptome prediction models from the UTMOST framework, hosted alongside JTI models; treated as a separate model set in this study [28] | 340,104 (tissues) | (49) |
| EpiXcan | https://www.synapse.org/Synapse:syn52745052 | Transcriptome imputation incorporating epigenomic annotations to weight SNP priors, improving prediction accuracy over standard elastic net [29] | 143,609 (tissues) | (14) |
| FUSION | http://gusevlab.org/projects/fusion/ | Bayesian sparse linear mixed model and penalized regression framework for transcriptome-wide association studies [17] | 265,052 (tissues) | (48) |
| TIGAR | https://github.com/yanglab-emory/TIGAR | Nonparametric Bayesian gene expression imputation tool supporting individual- and summary-level GWAS data for transcriptome-wide association studies [30] | 181,605 (tissues) | (49) |

missingness ≤ 0.1 and removal of related individuals using PLINK (`--rel-cutoff 0.125`) ([35, 36]).

Genetically Predicted Gene Expression

Genetically predicted gene expression was computed for each individual within each fold using PrediXcan-style genotype-based transcriptome imputation ([16, 18]), in which expression for gene g in tissue t is estimated as a weighted sum of SNP dosages using pre-trained expression-weight models. To maximize gene coverage and capture diverse regulatory architectures, we incorporated seven publicly available expression-weight databases trained under different statistical and biological assumptions: MASHR, JTI, CTIMP, UTMOST, EpiXcan, FUSION, and TIGAR (Table 1; full mathematical details are provided in Supplementary Methods S1). Predicted expression values were adjusted for sex and the top 10 genetic principal components using ordinary least squares regression applied to the training split only, with fitted parameters applied to validation and test splits.

Differential Expression Analysis

Differential expression analysis (DEA) was performed on covariate-adjusted imputed expression values for each gene, tissue, database, fold, and dataset split using eight statistical methods: LIMMA empirical Bayes moderated t -test ([37]), Welch’s unequal-variance t -test, OLS regression, Wilcoxon rank-sum test, phenotype-label permutation test ($B = 1,000$ permutations), weighted logistic regression, bias-reduced Firth logistic regression, and Bayesian logistic approximation. For differential-expression methods, significance required $FDR < 0.1$ and $|\log_2 FC| \geq 0.5$; for association-style methods, significance required $FDR < 0.1$ and $|\text{Effect}| \geq 0.5$. Complete model specifications are provided in Supplementary Methods S1.

Gene Prioritization

Significant genes were aggregated across all databases, tissues, folds, and methods. The discovery set was defined as $G_{\text{discovery}} = G_{\text{train}} \cup G_{\text{val}}$, reserving G_{test} exclusively for out-of-sample evaluation. Each gene in $G_{\text{discovery}}$ was scored using a composite importance score S_g that integrates three components: reproducibility (40%), effect magnitude (30%),

and statistical confidence (30%). Reproducibility captures both the total number of significant hits and the breadth of support across database-tissue-method combinations. Effect magnitude is derived from method-standardized absolute effect sizes. Statistical confidence is derived from BH-adjusted FDR values. Full scoring formulas are provided in Supplementary Methods S2. Rankings were robust to alternative weights (Spearman $\rho = 0.992$; Top-100 overlap $\geq 75\%$; full stability results in Supplementary Table S1).

Generalizability was assessed using the held-out test split as the replication target. For each gene g in the tested universe U , a binary label $y_g = \mathbb{I}(g \in G_{\text{test}})$ was defined, and S_g was used as the ranking predictor. Performance was quantified using ROC-AUC, PR-AUC, and hypergeometric enrichment tests at multiple top- K cutoffs. Enrichment for a curated set of 3,190 migraine-associated genes ([15]) assembled via `PhenotypeToGeneDownloaderR` (<https://github.com/MuhammadMuneeb007/PhenotypeToGeneDownloaderR>) was assessed using the same hypergeometric framework. Full test derivations are provided in Supplementary Methods S3.

To obtain an integrated target-prioritization ranking, S_g was combined with three additional evidence layers: pathway support (*PathwayScore*) derived from GO, KEGG, Reactome, and Disease Ontology enrichment analyses (`clusterProfiler`, `ReactomePA`, `DOSE`); network hub score from STRING protein-protein interaction analysis; and structure- or knowledge-based druggability from DGIdb, ChEMBL, and fpocket. The integrated score was computed as $\text{CoreScore}_g = 0.45 \cdot \text{DE}_g^{\text{norm}} + 0.25 \cdot \text{Path}_g^{\text{norm}} + 0.25 \cdot \text{Drug}_g^{\text{norm}} + 0.05 \cdot \text{Hub}_g^{\text{norm}}$, with DE weighted highest because it provides the primary TWAS-derived genetic link between genotype and disease. Full pathway score propagation formulas and weight justification are provided in Supplementary Methods S2.

Drug Repurposing

A curated migraine drug reference set of 4,824 normalized drug entries was assembled using `DownloadDrugsRelatedToDiseases` (<https://github.com/MuhammadMuneeb007/DownloadDrugsRelatedToDiseases>), which aggregates drug-disease associations from Open Targets, DrugBank, CTD, and literature-mining sources. All enrichment claims are framed relative to a global background of 139,597 drugs. Candidate compounds were mapped from the top N ranked genes using drug-target

evidence from Open Targets, DGIdb, and ChEMBL, with drug names harmonized using conservative text normalization. Each gene–drug evidence row was assigned an evidence weight based on clinical development stage, and a *DrugScore* was computed by aggregating $\text{GeneWeight} \times \text{EvidenceWeight}$ contributions across all supporting genes.

The curated migraine drug reference set was partitioned into four development-stage tiers: Tier 1 (migraine-specific approved therapies), Tier 2 (guideline-supported acute or preventive therapies), Tier 3 (established off-label therapies), and Tier 4 (broader literature-linked compounds). Performance was assessed using multi- K overlap evaluation under two complementary universes: an ALL-drugs global background (hypergeometric test valid) and a PREDICTED candidates-only universe (AUROC and AUPRC are the appropriate metrics; full results in Supplementary Table S5).

Directionality Assessment

To assess mechanistic compatibility of prioritized gene–drug pairs, drug action annotations were extracted from locally aggregated evidence fields and supplemented via ChEMBL and DGIdb, harmonized into a reduced action vocabulary (inhibitor, antagonist, agonist, activator, modulator, unknown). Each pair was classified as directionally consistent when the drug action was compatible with the inferred disease-associated gene direction, inconsistent when opposed, or unclear when insufficient annotation was available. Full annotation and classification criteria are provided in Supplementary Methods S4.

Results

Cross-database concordance of predicted gene expression

A total of 733 participants (53 cases, 680 controls) were stratified into five cross-validation folds, preserving case–control balance across training (80%), validation (10%), and test (10%) splits. Within each fold and split, we imputed genetically regulated expression from genotype dosages using PrediXcan-style models ([16, 18]).

To compare expression-weight databases, we quantified tissue-matched concordance by computing gene-wise Pearson correlations of predicted expression across individuals for genes shared by each database pair, then averaging within tissue and across folds to yield one concordance estimate per database pair and split. The highest concordance was observed for the CTIMP–UTMOST pair ($r \approx 0.55$; train = 0.547, validation = 0.546, test = 0.546), followed by JTI–CTIMP ($r \approx 0.53$; train = 0.526, validation = 0.525, test = 0.525), MASHR–UTMOST ($r \approx 0.54$; train = 0.536, validation = 0.538, test = 0.537), and MASHR–CTIMP ($r \approx 0.49$; train = 0.491, validation = 0.492, test = 0.492). Concordance with FUSION was moderate for UTMOST ($r \approx 0.50$; train = 0.498, validation = 0.497, test = 0.499) and lower for MASHR ($r \approx 0.38$; train = 0.380, validation = 0.380, test = 0.378) and JTI ($r \approx 0.31$; train = 0.311, validation = 0.310, test = 0.311). TIGAR showed near-zero concordance with all other databases ($r \approx 0.03$), indicating substantially different predicted-expression patterns (Figure 2).

Adjusting expression for sex and the top ten genetic principal components had negligible impact on cross-database correlations (overall mean $\Delta r = r_{\text{fixed}} - r_{\text{raw}} \approx -1 \times$

10^{-4}). However, the adjustment altered expression values modestly overall ($\text{corr}(\text{raw}, \text{fixed}) = 0.9696$, $\text{mean}|\Delta| = 0.00797$, $\text{RMSE} = 0.0353$), with the largest shifts observed in FUSION ($\text{mean}|\Delta| \approx 0.023$, $\text{RMSE} \approx 0.124$) and in EpiXcan ($\text{mean}|\Delta| \approx 0.011$, $\text{RMSE} \approx 0.078$), while TIGAR showed minimal absolute change ($\text{mean}|\Delta| \approx 6.3 \times 10^{-5}$). These results suggest that cross-database differences primarily reflect methodological and architectural variation among expression-weight resources, rather than confounding by sex or ancestry principal components.

Gene differential expression analysis

We performed 172,868,680 gene-level differential-expression and association tests across expression-weight databases, tissues, folds, dataset splits, and eight statistical methods. Applying the predefined significance and effect-size thresholds yielded 96,502 significant test records, corresponding to 11,451 unique significant genes within a tested universe of $U = 34,355$ genes. Given the modest cohort size and the highly layered testing design, these counts should be interpreted primarily as a broad discovery space rather than as a set of individually robust causal signals. Importantly, the main ranking conclusions were preserved under stricter thresholds in sensitivity analyses, indicating that the held-out prioritization signal does not depend solely on the most permissive operating point. Discovery candidates were defined without test leakage using training and validation only, producing $G_{\text{discovery}} = G_{\text{train}} \cup G_{\text{val}}$ ($n = 9,305$), of which 1,189 overlapped a curated migraine-linked reference set and 8,116 remained outside that reference space.

Out-of-sample replication was assessed by treating test-significant genes ($T = 7,141$) as positives within U , where $G_{\text{discovery}}$ recovered 4,995 test positives (recall = 0.699) with precision = 0.537, while smaller top- K lists achieved higher precision at the cost of recall (e.g., top-100 precision = 0.790; Table 2).

We next evaluated the continuous discovery score as a genome-wide ranking model over the full tested universe U , using test-significant genes ($T = 7,141$) as the replication target. Under this ranking framework, the score achieved ROC-AUC = 0.7753 and PR-AUC = 0.4754, indicating meaningful separation of test-replicating genes from non-replicating genes. Given the baseline prevalence of positives in the tested universe ($T/U = 0.2079$), the observed PR-AUC corresponds to a substantial lift over random ranking. We therefore interpret the primary signal of G2DR at this stage not as binary hit identification, but as the ability to order genes such that held-out positives are preferentially concentrated toward the top of the ranked list. This distinction is important in small, class-imbalanced settings, where prioritization quality is more informative than exact gene-list identity (Table 3, left panel).

As an orthogonal validation, we tested enrichment for curated migraine genes ($M = 3,190$) within U . $G_{\text{discovery}}$ contained 1,189 known genes (expected 864.01), corresponding to 1.38-fold enrichment ($p = 5.47 \times 10^{-40}$), indicating that the discovery set preferentially captures established migraine biology while retaining a large novel component (Table 3, right panel).

Together, these results show that integrating gene-level evidence across tissues, methods, and databases yields a reproducible prioritization that generalizes to held-out test data, performs substantially better than random ranking, and

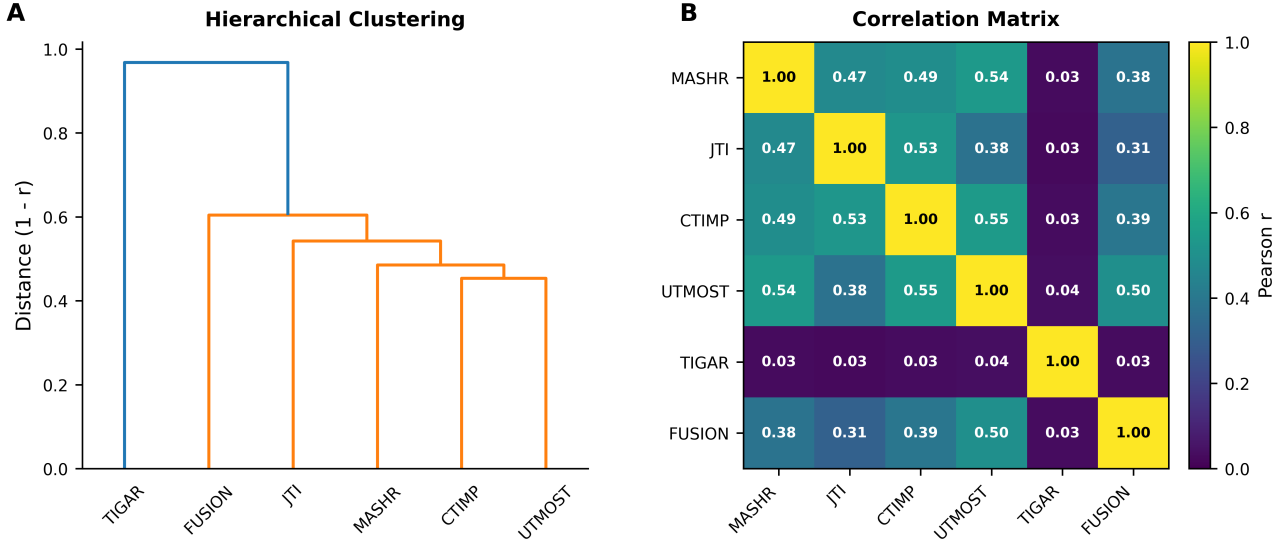


Fig. 2. Cross-database concordance of predicted gene expression across expression-weight databases. (A) Hierarchical clustering of databases using distance $(1 - r)$ derived from the pairwise correlation matrix. (B) Pairwise correlation matrix (Pearson r).

Table 2. Held-out test replication for the discovery set and top- K lists. Positives are test-significant genes ($T = 7,141$). TP/FP/FN are computed relative to T .

| Predicted set | TP | FP | FN | Precision | Recall |
|---|-------|-------|-------|-----------|--------|
| $G_{\text{discovery}}$ (train \cup val) | 4,995 | 4,310 | 2,146 | 0.537 | 0.699 |
| Top 50 | 39 | 11 | 7,102 | 0.780 | 0.005 |
| Top 100 | 79 | 21 | 7,062 | 0.790 | 0.011 |
| Top 200 | 156 | 44 | 6,985 | 0.780 | 0.022 |
| Top 500 | 347 | 153 | 6,794 | 0.694 | 0.049 |
| Top 1000 | 664 | 336 | 6,477 | 0.664 | 0.093 |

Table 3. Hypergeometric enrichment of predicted sets for held-out test positives and curated migraine genes. For test positives: $k_{\text{exp}} = N_{\text{pred}} \cdot (T/U)$, $T = 7,141$, $U = 34,355$. For migraine genes: $k_{\text{exp}} = N_{\text{pred}} \cdot (|M|/U)$, $|M \cap U| = 3,190$. FE = $k_{\text{obs}}/k_{\text{exp}}$.

| Set | Test positives ($T = 7,141$) | | | | | Curated migraine genes ($ M = 3,190$) | | | | |
|---|--------------------------------|------------------|------------------|------|-------------------------|--|------------------|------------------|------|------------------------|
| | N_{pred} | k_{obs} | k_{exp} | FE | p -value | N_{pred} | k_{obs} | k_{exp} | FE | p -value |
| $G_{\text{discovery}}$ (train \cup val) | 9,305 | 4,995 | 1,934.13 | 2.58 | $< 10^{-300}$ | 9,305 | 1,189 | 864.01 | 1.38 | 5.47×10^{-40} |
| Top 50 | 50 | 39 | 10.39 | 3.75 | 7.14×10^{-18} | 50 | 12 | 4.64 | 2.58 | 1.71×10^{-3} |
| Top 100 | 100 | 79 | 20.79 | 3.80 | 1.55×10^{-35} | 100 | 21 | 9.29 | 2.26 | 2.97×10^{-4} |
| Top 200 | 200 | 156 | 41.57 | 3.75 | 1.77×10^{-67} | 200 | 36 | 18.57 | 1.94 | 8.72×10^{-5} |
| Top 500 | 500 | 347 | 103.93 | 3.34 | 6.94×10^{-123} | 500 | 74 | 46.43 | 1.59 | 4.26×10^{-5} |
| Top 1000 | 1,000 | 664 | 207.86 | 3.19 | 2.30×10^{-220} | 1,000 | 132 | 92.85 | 1.42 | 2.39×10^{-5} |

can be further refined into compact candidate gene sets for downstream network and drug-mapping analyses.

Gene prioritization was robust to stricter significance thresholds

To assess whether the discovery-based prioritization was sensitive to the choice of significance threshold, we repeated the same workflow under stricter FDR and effect-size criteria. Relative to the primary analysis (FDR < 0.10 , $|\log_2 \text{FC}| \geq 0.50$), tightening the FDR threshold to < 0.05 reduced the number of significant genes in training, validation, and test from 1,046, 9,107, and 7,141 to 958, 7,861, and 5,313, respectively, and reduced $G_{\text{discovery}}$ from 9,305 to 8,135 genes. Increasing the effect-size threshold to $|\log_2 \text{FC}| \geq 0.75$ at FDR

< 0.10 reduced these counts further to 263, 6,241, and 4,599 genes, yielding $G_{\text{discovery}} = 6,303$, while the strictest setting (FDR < 0.05 , $|\log_2 \text{FC}| \geq 0.75$) produced 248 training genes, 5,709 validation genes, and 3,772 test genes, with $G_{\text{discovery}} = 5,794$.

Despite the expected reduction in $G_{\text{discovery}}$ size under stricter filtering, held-out replication remained substantial across all threshold settings. The primary analysis achieved ROC-AUC = 0.7753 and PR-AUC = 0.4754. Under FDR < 0.05 and $|\log_2 \text{FC}| \geq 0.50$, performance remained above random with ROC-AUC = 0.7314 and PR-AUC = 0.3412. Under the stricter effect-size threshold of $|\log_2 \text{FC}| \geq 0.75$, performance was similarly retained, with ROC-AUC = 0.7339 and PR-AUC = 0.3289 for FDR < 0.10 , and ROC-AUC

= 0.7025 and PR-AUC = 0.2497 for FDR < 0.05. $G_{\text{discovery}}$ also remained strongly enriched for held-out test positives across all settings, with fold enrichment ranging from 2.58-fold to 3.20-fold. Enrichment for curated migraine genes was likewise preserved, ranging from 1.38-fold under the primary rule to 1.41-fold under the strictest setting. Full sensitivity results are provided in Supplementary Table S2; together, these results indicate that the main gene-prioritization findings are not driven by permissive significance filtering.

Component-based recovery

To identify which components contributed the most disease-relevant signal in $G_{\text{discovery}}$, we tested whether each component-specific discovery set (defined using training and validation only) was enriched for curated migraine-associated genes. For each database, tissue, and method, we defined a discovery set as the unique genes that were significant at least once within that component across folds and the remaining dimensions, and quantified over-representation of database-annotated migraine-linked genes using a fold-enrichment statistic ($FE = k_{\text{obs}}/k_{\text{exp}}$) with empirical p -values from size-matched random gene-set sampling. Full results across all databases, tissues, and methods are provided in Supplementary Table S3.

Across expression-weight databases, MASHR showed the strongest discovery enrichment ($FE = 2.30$, $p_{\text{emp}} = 1 \times 10^{-4}$), followed by JTI ($FE = 1.86$, $p_{\text{emp}} = 6.799 \times 10^{-3}$) and FUSION ($FE = 1.36$, $p_{\text{emp}} = 1 \times 10^{-4}$), whereas EpiXcan, CTIMP, UTMOST, and TIGAR showed weaker and non-significant enrichment. Across tissues, discovery enrichment highlighted a reproducible set of migraine-informative contexts, led by Brain Amygdala ($FE = 1.96$, $p_{\text{emp}} = 1 \times 10^{-4}$), Minor Salivary Gland ($FE = 1.94$, $p_{\text{emp}} = 1 \times 10^{-4}$), and Whole Blood ($FE = 1.83$, $p_{\text{emp}} = 1 \times 10^{-4}$), with multiple additional tissues showing significant over-representation of database-annotated migraine-linked genes. Across methods, the discovery signal was dominated by the association-style models: Weighted Logistic and Bayesian Logistic both showed consistent enrichment ($FE \approx 1.37$, $p_{\text{emp}} = 1 \times 10^{-4}$), while Welch t -test identified a smaller, disease-dense set ($FE = 1.35$, $p_{\text{emp}} = 6 \times 10^{-4}$); low-coverage methods did not show significant discovery enrichment.

Unified gene prioritization framework

We next evaluated a unified gene-prioritization framework by comparing individual evidence components against both the primary composite score and the multi-source integrated score. Two complementary evaluation universes were used throughout. The **full universe** comprised all $U = 34,355$ tested genes; genes not in the discovery set received a score of zero, so this universe measures how well a ranking separates discovery-relevant genes from the entire tested space — the same universe used to compute the headline ROC-AUC and PR-AUC reported above. The **discovery universe** comprised only the $n = 9,305$ genes in $G_{\text{discovery}}$ (train \cup val); here non-discovery genes are absent, so this universe measures ranking quality *within* the already-selected candidates — a strictly harder question.

Two composite scores were evaluated. The **primary composite score** (S_g , *Importance.Score*) integrates reproducibility, effect magnitude, and statistical confidence with weights 40/30/30. The **integrated score** additionally combines S_g with pathway support, druggability evidence, and network hub

score (weights DE = 0.45, Pathway = 0.25, Drug = 0.25, Hub = 0.05), and is designed for downstream target selection.

Evaluated over all 34,355 tested genes, effect-only ranking achieved the strongest test-replication performance (ROC-AUC = 0.790, PR-AUC = 0.526), marginally exceeding the primary composite (ROC-AUC = 0.775, PR-AUC = 0.475) and the integrated score (ROC-AUC = 0.776, PR-AUC = 0.472). The elevated AUC values across most rankings in this universe reflect the large separation between discovery genes (score > 0) and the majority of non-discovery genes (score = 0), rather than solely fine-grained within-set discrimination. For curated migraine-gene enrichment at Top-200, pathway ranking recovered 66 known genes ($FE = 3.55$, precision = 0.330) and hub ranking recovered 64 ($FE = 3.45$, precision = 0.320), both substantially exceeding the primary composite (36 genes; $FE = 1.94$) and significance-only (25 genes; $FE = 1.35$) rankings.

Within $G_{\text{discovery}}$ alone, effect-only ranking remained the strongest for test replication (ROC-AUC = 0.675, PR-AUC = 0.663), recovering 145 held-out test-positive genes at Top-200. The primary composite and significance-only rankings showed similar within-set replication (ROC-AUC \approx 0.54–0.55), indicating that the headline 0.775 figure is driven in substantial part by discovery-versus-non-discovery separation rather than by within-set ranking quality alone. Pathway and hub rankings showed substantially stronger enrichment for curated migraine biology: at Top-200, pathway ranking recovered 66 database-annotated migraine-linked genes ($FE = 2.58$, precision = 0.330) and hub ranking recovered 64 ($FE = 2.50$, precision = 0.320). Direct target evidence recovered 58 known genes ($FE = 2.27$, precision = 0.290), whereas drug-link count and druggability alone provided weaker standalone biological enrichment.

Component-level benchmarking showed that no single evidence layer was uniformly optimal across all evaluation criteria. Effect-only ranking performed best for held-out replication, whereas pathway- and hub-based rankings were stronger for enrichment of curated migraine biology. The integrated score therefore should not be interpreted as maximizing any single benchmark metric; rather, it represents a balanced operating point designed for downstream target selection, where replication support, biological coherence, and translational tractability all matter simultaneously. In this sense, the value of integration lies in controlled trade-off rather than empirical dominance on one axis alone. Full component-wise metrics across both universes are provided in Supplementary Table S4.

To assess whether the integrated score weights were arbitrary, we evaluated 17 alternative weighting schemes spanning nine reasonable alternatives (e.g. DE-heavy, pathway-heavy, drug-heavy, equal, and no-hub variants) and eight extreme stress tests (single-component schemes). Across reasonable alternatives, the mean Spearman ρ against the default ranking was 0.963 (minimum 0.866), with a mean Top-100 gene overlap of 81.6%; crucially, performance metrics were virtually unchanged, with DISC-universe test ROC-AUC ranging only from 0.544 to 0.547 and FULL-universe test ROC-AUC from 0.775 to 0.776 across all nine schemes (Supplementary Table S1). Extreme single-component schemes diverged substantially (mean $\rho = 0.682$, minimum 0.292 for hub-only), suggesting that the integrated score draws on genuine multi-source signal rather than being dominated by any single layer. These results suggest that the default weights (DE = 0.45, Pathway = 0.25, Drug = 0.25, Hub = 0.05) lie within a stable region of parameter space, with divergence occurring

only under extreme parameterizations that lack biological justification in a TWAS-first pipeline.

Significant gene comparison against Open Targets

We compared G2DR with the Open Targets migraine disease-target resource using the same curated migraine reference set ($M = 3,190$ genes). In the full analysis, G2DR ranked 9,305 genes across the broader genotype-first search space, whereas Open Targets returned 2,376 migraine-associated targets. The full G2DR ranking recovered 1,189 curated migraine genes (37.27%), while Open Targets recovered 1,228 (38.50%), and G2DR additionally recovered 725 curated migraine reference genes absent from Open Targets entirely. When G2DR was restricted to genes represented in the Open Targets target space ($n = 823$), Top-50 precision increased from 22.00% to 46.00% and Top-200 precision increased from 23.00% to 55.50%, approaching but not matching the standalone Open Targets precision (Top-50: 92.00%), which reflects its disease-curated, pre-filtered design rather than a direct performance comparison. Full comparison metrics are provided in Supplementary Table S6. These comparisons are complementary rather than directly competitive: Open Targets offers higher precision within a curated space, while G2DR extends target hypothesis generation beyond existing disease annotations, recovering a substantial set of curated migraine reference genes that are absent from Open Targets entirely.

Drug mapping and candidate enrichment

Using the ranked migraine gene lists (top $N = 200$ and $N = 500$), we aggregated gene-drug evidence from Open Targets, DGIdb, and ChEMBL to generate ranked candidate compounds. For $N = 200$, the pipeline compiled 5,348 gene-drug evidence rows and yielded 3,963 unique predicted drugs. For $N = 500$, evidence increased to 11,234 rows and the predicted set expanded to 7,981 unique drugs.

We evaluated overlap with a curated reference set of 4,824 normalized migraine-associated drugs under two complementary evaluation frames. First, an **ALL-drugs universe** (139,597 background drugs) tests capture and enrichment: whether the returned candidates include migraine-linked drugs above chance relative to the global pharmacopeia. Second, a **PREDICTED universe** (3,963 or 7,981 returned drugs) evaluates ranking within the returned candidate set: whether reference migraine-associated drugs are preferentially placed toward the top among returned compounds. Note that FE values below 1.0 in the PREDICTED universe reflect the fact that the reference migraine drug set exceeds the returned candidate pool in size, making standard hypergeometric enrichment interpretation inapplicable in that frame; AUROC and AUPRC are the appropriate metrics for within-set ranking performance.

Under the ALL-drugs background, both gene sets showed strong enrichment of known migraine drugs. For $N = 200$, recovery increased from 5/20 (Precision@20 = 0.25, FE = 7.23, $p = 4.93 \times 10^{-4}$) to 51/100 (Precision@100 = 0.51, FE = 14.76, $p = 4.20 \times 10^{-47}$) and 205/500 (Precision@500 = 0.41, FE = 11.86, $p = 6.19 \times 10^{-161}$). For $N = 500$, early enrichment improved further (8/20, Precision@20 = 0.40, FE = 11.58, $p = 1.75 \times 10^{-7}$; 53/100, Precision@100 = 0.53, FE = 15.34, $p = 4.48 \times 10^{-50}$; 213/500, Precision@500 = 0.426, FE = 12.33, $p = 1.67 \times 10^{-171}$). These results indicate that both gene inputs yield drug sets highly enriched for established migraine-relevant compounds relative to a global drug background.

Within the returned candidates, for $N = 200$, 353 curated migraine drugs were present among 3,963 predicted drugs and the ranking achieved AUROC = 0.8004 and AUPRC = 0.3528. For $N = 500$, 527 curated migraine drugs were present among 7,981 predicted drugs with AUROC = 0.8152 and AUPRC = 0.3311. Expanding the input from 200 to 500 genes increased the number of recovered reference drugs and modestly improved AUROC, while AUPRC decreased slightly due to the larger candidate universe. Together, the two-universe evaluation separates capture from ranking: the strong fold-enrichment and hypergeometric significance under the ALL universe supports disease-relevant signal in the upstream gene prioritization, while AUROC and AUPRC suggest that reference migraine-associated drugs tend to appear earlier than non-reference drugs within the returned set. Full multi- K overlap results for both $N = 200$ and $N = 500$ under both universes are provided in Supplementary Table S5.

When we mapped the predicted drug set back to disease indications in the aggregated drug-disease database, migraine was not always the top recovered indication. Instead, cardiometabolic, inflammatory, neuropsychiatric, and seizure-related categories frequently ranked highly. This is biologically plausible because migraine has a well-established comorbidity landscape and shares mechanisms, risk factors, and therapeutic overlap with multiple neurological and systemic disorders ([31, 32, 33, 34]). Disease-label recovery should therefore be interpreted as reflecting shared pharmacology and overlapping biology across comorbid conditions rather than as a migraine-exclusive signal. We partitioned the curated migraine drug reference set ($n = 4,824$ normalized drugs) into four evidence-oriented tiers: migraine-specific approved therapies (Tier 1; triptans, ditans, gepants, CGRP monoclonals, ergot derivatives), guideline-supported acute or preventive therapies (Tier 2), established off-label therapies (Tier 3), and broader literature-linked compounds (Tier 4). Recovery of each tier was evaluated within the ranked candidate drug list against a global background of 139,597 drugs.

Across the pooled migraine-drug reference set, the ranked list recovered migraine-linked compounds at rates above random expectation, but tiered evaluation showed that this recovery was uneven across evidence classes. No Tier 1 migraine-specific approved therapies were recovered within the Top-200 ranked drugs, whereas overlap was more evident for guideline-supported, off-label, and broader literature-linked compounds. These results indicate that the current framework is better at surfacing broader mechanism-linked and repurposing-relevant pharmacology than at rediscovering the most migraine-specific modern therapeutic classes. We therefore interpret the drug-level signal as evidence of biologically meaningful translational expansion rather than indication-specific clinical precision (Table 4).

Directionality of prioritized gene-drug pairs

To assess mechanistic plausibility beyond drug enrichment alone, we evaluated the directionality of all gene-drug pairs derived from the top 200 genes of the final integrated migraine ranking. Across 4,861 unique gene-drug pairs, 549 (11.3%) were classified as directionally consistent, 618 (12.7%) as inconsistent, and 3,694 (76.0%) as unclear (Table 5). When restricted to the 614 pairs involving drugs from the curated migraine reference set, 50 (8.1%) were consistent, 83 (13.5%) inconsistent, and 481 (78.3%) unclear. The proportions were broadly stable across both universes, indicating that

Table 4. Tiered migraine-evidence benchmark of the ranked drug list. Tier 1: migraine-specific approved therapies ($n_{\text{ref}} = 135$); Tier 2: guideline-supported therapies ($n_{\text{ref}} = 92$); Tier 3: established off-label therapies ($n_{\text{ref}} = 29$); Tier 4: broader literature-linked compounds ($n_{\text{ref}} = 4,568$). Fold enrichment (FE) and hypergeometric p -values are computed relative to a global background of 139,597 drugs. High FE values for Tiers 2-3 reflect low absolute counts and should be interpreted accordingly.

| Tier | Top-20 | Top-50 | Top-100 | Prec@100 | Rec@100 | FE@100 | $p@100$ | Top-200 |
|------------------------------------|--------|--------|---------|----------|---------|--------|------------------------|---------|
| Tier 1: Migraine-specific approved | 0 | 0 | 0 | 0.00 | 0.000 | 0.00 | 1.00 | 0 |
| Tier 2: Guideline-supported | 0 | 1 | 2 | 0.02 | 0.022 | 30.35 | 2.04×10^{-3} | 2 |
| Tier 3: Established off-label | 1 | 1 | 1 | 0.01 | 0.034 | 48.14 | 2.06×10^{-2} | 1 |
| Tier 4: Broad literature-linked | 4 | 18 | 48 | 0.48 | 0.011 | 14.67 | 7.08×10^{-44} | 86 |

the directionality signal does not selectively concentrate in migraine-annotated compounds.

Among the 50 directionally consistent migraine-drug pairs, several biologically interpretable clusters emerged. First, aspirin-*GSTP1* (drug rank 26; *GSTP1* higher in cases) was classified as consistent based on a ChEMBL inhibitor annotation; this pair should be interpreted with caution because aspirin’s primary mechanism is COX-1/COX-2 inhibition, and the *GSTP1* annotation likely reflects indirect or in vitro effects rather than direct pharmacological inhibition. Second, the cardiac glycosides digoxin and digitoxin (drug ranks 126 and 133) were consistent against *ATP1A4* (higher in cases; gene rank 2), which encodes a Na^+/K^+ -ATPase $\alpha 4$ subunit; cardiac glycosides are established Na^+/K^+ -ATPase inhibitors, making the directionality pharmacologically coherent, though *ATP1A4* itself is supported by only a single-family case report in migraine and should be considered a low-evidence candidate gene rather than an established migraine locus. Third, several GLP-1 receptor agonists (exenatide, liraglutide, semaglutide, lixisenatide; drug ranks 142–146) were mapped against *ALPL* (lower in cases; gene rank 6) via DGIdb annotations; this mapping should be interpreted cautiously because GLP-1 agonists act canonically through GLP1R rather than *ALPL* directly, and the annotation likely reflects indirect effects on alkaline phosphatase activity rather than direct pharmacological agonism. Fourth, α_1 -adrenergic receptor antagonists including phenoxybenzamine, phentolamine, prazosin, and carvedilol (drug ranks 377–551) were consistent against *ADRA1A* (higher in cases; gene rank 150), where inhibition of elevated adrenergic signalling is mechanistically plausible. Fifth, amitriptyline (drug rank 438; a guideline-supported migraine prophylactic) showed consistent directionality against *AADAC* (higher in cases; gene rank 119) via DGIdb inhibitor annotations.

Directionality filtering materially refined the candidate space by separating broadly recovered compounds from those with stronger mechanistic compatibility. Among migraine-linked or biologically plausible candidates, only a subset remained directionally consistent, while others were directionally inconsistent or unresolved because the mapped action did not align clearly with the inferred disease-associated gene direction. This distinction matters because enrichment alone can recover compounds that are pharmacologically adjacent to migraine biology without necessarily supporting a coherent repurposing hypothesis. Accordingly, we treat directionally consistent pairs as higher-priority computational hypotheses, whereas inconsistent or unresolved pairs should be viewed as context signals rather than actionable leads.

Top gene and drug validation panel

To provide a concise summary of the final integrated prioritization, we assembled top-gene and top-drug evidence

panels from the *Combined_Score*-ranked gene list and the downstream drug-mapping and directionality outputs. The top-gene panel (Table 7) reports the 10 highest-ranked genes together with their evidence support, inferred disease direction, migraine relevance, and linked druggability information. The top-drug panel (Table 8) reports the 10 highest-ranked drugs with merged target gene information, approval status, and directionality classification.

Top gene highlights.

Among the top 10 integrated-score genes, *ATP1A4* (rank 2; higher in cases; known migraine gene; 24 linked drugs; Consistent directionality) was the most directly disease-relevant, encoding the Na^+/K^+ -ATPase $\alpha 4$ subunit and linking to cardiac glycoside inhibitors including digoxin and digitoxin. *ALPL* (rank 6; lower in cases; Tier 1 confidence; 96 linked drugs; Consistent) was the most druggable top gene, linked to GLP-1 agonists through DGIdb annotations. *HLA-DQB1* (rank 3; lower in cases; known migraine gene; 55 linked drugs) had the broadest drug connectivity but showed inconsistent directionality. *MRPL36* (rank 18; higher in cases; 67 linked drugs; Consistent) was linked to a cluster of antibiotic and antimicrobial drugs through mitochondrial ribosomal inhibition annotations. Among the 49 database-annotated migraine-linked genes present in the top 200, additional highly ranked examples included *GSTP1* (rank 31; Consistent; aspirin-*GSTP1* was the most evidenced approved consistent pair), *GRIN2B* (rank 44; 110 linked drugs; known migraine gene), and *OSGEP* (rank 58; highest composite *Importance_Score* of 0.682; known migraine gene). Several top-ranked genes — including *GRHPR*, *MRPL21*, *DHX15*, and *GCDH* — had few or no linked drugs.

Top drug highlights.

Among the top 10 ranked drugs, lifitegrast (rank 6; approved; targets *ITGB2* and *ICAM1*, both higher in cases; Consistent) was the only approved drug in the top 10 with directional consistency, acting as an integrin inhibitor compatible with elevated integrin subunit expression. Oleclumab (rank 12; Phase 3; targets *NT5E*; Consistent) and ezatiostat (rank 13; Phase 2; targets *GSTP1*; Consistent) provided the clearest non-approved consistent candidates. Neramexane (rank 17; Phase 3; targets *GRIN2B* and *CHRNA10*; Consistent) was the highest-ranking investigational drug with a migraine-biology rationale through NMDA receptor modulation. Several top-ranked approved drugs showed directionally inconsistent mappings, including metformin (rank 2; Inconsistent against *NDUFV1* and *NDUFS6*), amantadine (rank 5; Inconsistent against *GRIN2B*), diboterminalfa (rank 4; Inconsistent against *BMPR1B*), and apremilast (rank 10; Inconsistent against *PDE4C*). Among the top 20 migraine-reference drugs, aspirin (rank 26; Consistent against *GSTP1*) was the highest-ranking approved drug with directional support, while metformin, esketamine, and memantine appeared at ranks 2, 7, and 8

Table 5. Summary of directionality classification for unique prioritized gene–drug pairs from the final integrated migraine ranking. Results are shown for all pairs derived from the top 200 ranked genes and separately for pairs involving drugs from the curated migraine reference set ($n_{\text{mig}} = 614$).

| Directionality class | All pairs ($n = 4,861$) | | Migraine drugs only ($n = 614$) | |
|----------------------|---------------------------|--------|-----------------------------------|--------|
| | Count | % | Count | % |
| Consistent | 549 | 11.3% | 50 | 8.1% |
| Inconsistent | 618 | 12.7% | 83 | 13.5% |
| Unclear | 3,694 | 76.0% | 481 | 78.3% |
| Total | 4,861 | 100.0% | 614 | 100.0% |

Table 6. Representative directionally consistent gene–drug pairs from the migraine reference set. Pairs were classified as consistent when the known drug action was mechanistically compatible with the inferred disease-associated direction of the target gene. Drug rank is from the integrated gene-to-drug scoring pipeline; gene rank is from the *Combined_Score* integrated gene prioritization. Evidence source indicates the database providing mechanism-of-action annotation. The *MRPL36* antibiotic cluster (rows 3–9) reflects DGIdb-derived mitochondrial ribosomal inhibitor annotations and should be interpreted with caution.

| Drug rank | Drug | Gene | Gene rank | Disease direction | Drug action | Evidence source | Approved | Known migraine gene |
|-----------|-----------------|--------|-----------|-------------------|-------------|-----------------|----------|---------------------|
| 26 | Aspirin | GSTP1 | 31 | Higher in cases | Inhibitor | ChEMBL | Yes | Yes |
| 126 | Digoxin | ATP1A4 | 2 | Higher in cases | Inhibitor | DGIdb | Yes | Yes |
| 133 | Digitoxin | ATP1A4 | 2 | Higher in cases | Inhibitor | DGIdb | Yes | Yes |
| 142 | Exenatide | ALPL | 6 | Lower in cases | Agonist | DGIdb | Yes | No |
| 144 | Liraglutide | ALPL | 6 | Lower in cases | Agonist | DGIdb | Yes | No |
| 146 | Semaglutide | ALPL | 6 | Lower in cases | Agonist | DGIdb | Yes | No |
| 54 | Chloramphenicol | MRPL36 | 18 | Higher in cases | Inhibitor | DGIdb | Yes | No |
| 86 | Minocycline | MRPL36 | 18 | Higher in cases | Inhibitor | DGIdb | Yes | No |
| 162 | Clarithromycin | MRPL36 | 18 | Higher in cases | Inhibitor | DGIdb | Yes | No |
| 379 | Prazosin | ADRA1A | 150 | Higher in cases | Inhibitor | DGIdb | Yes | Yes |
| 512 | Carvedilol | ADRA1A | 150 | Higher in cases | Inhibitor | DGIdb | Yes | Yes |
| 438 | Amitriptyline | AADAC | 119 | Higher in cases | Inhibitor | DGIdb | Yes | No |
| 257 | Empagliflozin | SLC5A2 | 45 | Higher in cases | Inhibitor | DGIdb | Yes | No |
| 222 | Glycine | GRIN2B | 44 | Lower in cases | Agonist | DGIdb | Yes | Yes |
| 497 | Loxapine | KCNT1 | 133 | Lower in cases | Activator | DGIdb | Yes | Yes |

Table 7. Top 10 prioritized genes from the final integrated migraine ranking. Genes are ranked by *Combined_Score* (integrated: DE + pathway + druggability + hub). KnMig = known migraine gene; Tier = confidence tier from primary composite ranking; NDrugs = number of unique linked drugs; ApprDrug = has at least one approved linked drug; DirBest = best directionality support across linked drug pairs.

| Rank | Symbol | CombScore | ImpScore | Disease direction | KnMig | Confidence tier | Hits | Tissues | DBs | NDrugs | ApprDrug | DirBest |
|------|----------|-----------|----------|-------------------|-------|-------------------|------|---------|-----|--------|----------|--------------|
| 1 | APOBEC3G | 0.936 | 0.435 | Higher in cases | No | Tier3_Exploratory | 100 | 29 | 1 | 98 | Yes | Unclear |
| 2 | ATP1A4 | 0.934 | 0.531 | Higher in cases | Yes | Tier3_Exploratory | 18 | 3 | 3 | 24 | Yes | Consistent |
| 3 | HLA-DQB1 | 0.933 | 0.410 | Lower in cases | Yes | Tier2_Moderate | 32 | 15 | 2 | 55 | Yes | Inconsistent |
| 4 | PSMB5 | 0.932 | 0.413 | Lower in cases | No | Tier2_Moderate | 40 | 13 | 2 | 33 | Yes | Inconsistent |
| 5 | SLC1A1 | 0.932 | 0.491 | Lower in cases | No | Tier2_Moderate | 103 | 15 | 2 | 54 | Yes | Inconsistent |
| 6 | ALPL | 0.931 | 0.412 | Lower in cases | No | Tier1_High | 35 | 5 | 1 | 96 | Yes | Consistent |
| 7 | AQP5 | 0.930 | 0.419 | Lower in cases | No | Tier2_Moderate | 42 | 10 | 2 | 29 | Yes | Consistent |
| 8 | CBL | 0.930 | 0.385 | Unclear | No | Tier3_Exploratory | 4 | 2 | 1 | 29 | Yes | Unclear |
| 9 | GRHPR | 0.929 | 0.485 | Higher in cases | No | Tier3_Exploratory | 206 | 16 | 1 | 2 | No | Unclear |
| 10 | MRPL21 | 0.929 | 0.447 | Higher in cases | Yes | Tier2_Moderate | 93 | 31 | 1 | 1 | No | Unclear |

respectively, consistent with their presence in the migraine drug compendium.

Biological interpretation of prioritised genes and drug repurposing candidates

The 200 genes prioritised by the integrated G2DR pipeline converged on several biological themes with established or plausible relevance to migraine pathophysiology. Of these, 49 (24.5%) had prior evidence linking them to migraine or closely related headache phenotypes based on database annotation from OMIM, DisGeNET, and HPO, whereas the remainder represent computationally prioritized candidates without established migraine association. These novel signals should be treated as hypothesis-generating outputs of the prioritization pipeline rather than validated migraine targets,

and their biological interpretation below is offered to motivate experimental follow-up rather than to make mechanistic claims. Overall, the prioritised genes mapped to pathways related to glutamatergic and ion-channel excitability, mitochondrial and metabolic function, immune and inflammatory signalling, cerebrovascular and extracellular-matrix integrity, and broader neuronal and synaptic maintenance, consistent with the multifactorial biology highlighted by large migraine genetic studies [38, 39].

Among the most interpretable signals, *GRIN2B* and *SLC1A1* supported glutamatergic hyperexcitability and cortical-spreading-depression-related biology [40, 41], while *SCN1B*, *KCNT1*, *KCNS2*, and *ATP1A4* pointed to broader disturbance of ion-channel homeostasis and neuronal firing. A second major component comprised mitochondrial and metabolic genes,

Table 8. Top 10 prioritized drug candidates from the final integrated migraine repurposing analysis. Drugs are ranked by *DrugScore*; target genes are merged per drug. KnMig = drug present in curated migraine reference set; NTarg = number of unique target genes among top 200; Dir = best directionality classification across gene–drug pairs.

| Rank | Drug | Phase | KnMig | Approved | NTarg | Target genes | Disease directions | Directionality | Evidence sources |
|------|-----------------|----------|-------|----------|-------|--|--------------------|----------------|--------------------|
| 1 | Ataluren | APPROVED | No | Yes | 4 | RPL28, RPS16 | Unclear, lower | Unclear | DGIdb, OpenTargets |
| 2 | Metformin | APPROVED | Yes | Yes | 2 | NDUFV1, NDUFS6 | Lower in cases | Inconsistent | OpenTargets, DGIdb |
| 3 | Voxelotor | APPROVED | No | Yes | 1 | HBB | Lower in cases | Unclear | OpenTargets |
| 4 | Dibotermin alfa | APPROVED | No | Yes | 1 | BMPR1B | Higher in cases | Inconsistent | OpenTargets |
| 5 | Amantadine | APPROVED | No | Yes | 1 | GRIN2B | Lower in cases | Inconsistent | OpenTargets |
| 6 | Lifitegrast | APPROVED | No | Yes | 2 | ITGB2, ICAM1 | Higher in cases | Consistent | OpenTargets |
| 7 | Esketamine | APPROVED | Yes | Yes | 1 | GRIN2B | Lower in cases | Unclear | OpenTargets, DGIdb |
| 8 | Memantine | APPROVED | Yes | Yes | 1 | GRIN2B | Lower in cases | Unclear | OpenTargets, DGIdb |
| 9 | Midostaurin | APPROVED | No | Yes | 7 | CBL, BMPR1B, CDK3, LATS2, PRKD3, SEPTIN9, PEG3 | Mixed | Inconsistent | OpenTargets, DGIdb |
| 10 | Apremilast | APPROVED | No | Yes | 1 | PDE4C | Lower in cases | Inconsistent | OpenTargets |

including *NDUFV1*, *NDUFS6*, *MRPL21*, *MRPL36*, *TUFM*, *VAR2*, *FXN*, *ETFB*, *COASY*, and *HAAO*, consistent with longstanding hypotheses that impaired cerebral bioenergetics contributes to migraine susceptibility [42, 43]. Immune and inflammatory signals were also prominent, including multiple HLA-region genes together with *RELA*, *ICAM1*, *CLEC7A*, *LY96*, *UNC93B1*, and *SERPINE1*, in keeping with evidence that neuroinflammatory and immune-trafficking mechanisms contribute to trigeminovascular sensitisation [44, 45, 46]. In parallel, neurovascular and extracellular-matrix genes such as *HTRA1*, *HSPG2*, *GNAQ*, *TIE1*, *EGFL7*, *LAMB1*, *F12*, and multiple collagen-related genes supported a vascular-integrity component, consistent with the broader overlap between migraine and cerebral small-vessel or neurovascular disorders [47, 48, 49]. Together, these results suggest that the prioritised set reflects convergence across excitability, metabolism, inflammation, and neurovascular maintenance rather than a single dominant molecular pathway.

The downstream drug-mapping analysis likewise recovered a broad migraine-relevant pharmacological landscape rather than only migraine-specific therapies. Using the top 200 genes, the pipeline identified 3,963 unique candidate drugs from 5,348 gene–drug evidence rows, and 353 curated migraine-associated drugs were present within the predicted set. Enrichment against the global drug background was strong, indicating that the upstream gene prioritisation captures disease-relevant pharmacology even though the output did not capture classical migraine medications. At the top of the ranked list, several recovered migraine-linked drugs were already notable, including metformin (rank 2), esketamine (rank 7), memantine (rank 8), aspirin (rank 26), dexamethasone (rank 48), lidocaine (rank 66), zonisamide (rank 79), indomethacin (rank 85), and acetaminophen (rank 98). Additional recovered migraine-associated or migraine-relevant drugs were present lower in the ranked set, including verapamil (rank 213), valproic acid (rank 253), celecoxib (rank 340), diclofenac (rank 343), amitriptyline (rank 438), topiramate (rank 491), and ergotamine tartrate (rank 521), showing that the pipeline recovered both acute-care and preventive classes as well as broader off-label and mechanism-linked therapies [50, 51, 52, 53, 54, 55, 56, 57].

Directionality filtering was particularly useful for separating broadly recovered drugs from those with clearer mechanistic compatibility. Among migraine-linked drugs, aspirin showed consistent directionality at *GSTP1*; amitriptyline was

directionally consistent at *AADAC*; and a cluster of antibiotic-derived mappings including chloramphenicol, minocycline, clarithromycin, erythromycin, tigecycline, and tobramycin were directionally consistent through *MRPL36*, although these latter signals should be interpreted cautiously because they arise from mitochondrial ribosomal annotations rather than direct migraine therapeutic use. Several non-reference but biologically interesting candidates were also directionally consistent as computational hypotheses, including lifitegrast at the *ITGB2–ICAM1* axis, neramexane at *GRIN2B/CHRNA10*, digoxin and digitoxin at *ATP1A4*, and GLP-1 receptor agonists such as exenatide, liraglutide, and semaglutide, mapped to *ALPL* via an indirect DGIdb annotation (GLP-1 agonists act canonically through *GLP1R* rather than *ALPL* directly); notably, GLP-1 agonists have shown promising signals in emerging clinical reports of chronic migraine management [58, 59, 60, 61], although all such pairs require direct experimental and clinical validation before any repurposing conclusions can be drawn. By contrast, several high-ranking recovered migraine drugs were directionally inconsistent, including metformin at *NDUFV1/NDUFS6*, dipyrindamole at *PDE4C*, carbamazepine, zonisamide, eslicarbazepine, oxcarbazepine, phenytoin, and lidocaine at *SCN5A*, as well as verapamil in its mapped targets. Other prominent recovered drugs, including esketamine, memantine, dexamethasone, indomethacin, acetaminophen, and valproic acid, were retained but remained directionally unresolved. Overall, these results indicate that the G2DR framework recovers a substantial set of migraine-relevant compounds, but that directional filtering is necessary to distinguish broadly associated drugs from those with stronger mechanistic coherence for repurposing. Taken together, the drug-mapping results suggest that G2DR is currently strongest as a framework for broad genetics-anchored translational hypothesis generation. It expands beyond curated disease-target space, recovers migraine-linked pharmacology above background, and benefits from directionality-aware refinement, but it does not yet recover migraine-specific approved therapies with high fidelity. This operating profile is consistent with a framework designed for prioritization and follow-up rather than definitive repurposing recommendation.

Discussion

We present G2DR as a genotype-first computational prioritization framework for settings in which genotype and phenotype labels are available but matched disease transcriptomics are limited or absent. The principal contribution is not a new TWAS algorithm or a clinically actionable target-identification system, but a modular workflow that converts inherited genetic signal into ranked target and compound hypotheses through multiple complementary evidence layers. In a migraine proof-of-concept, the framework generalized to held-out data at the gene-prioritization stage, recovered established migraine biology, and produced drug candidate sets enriched for migraine-linked pharmacology relative to a global background. Framed in this way, G2DR is best understood as a structured computational engine for narrowing the candidate space for downstream experimental and translational follow-up.

Several features of the results are especially informative. First, transcriptome-prediction resources were only moderately concordant, reinforcing that genetically predicted expression is itself model-dependent and that no single reference architecture should be assumed sufficient. Second, component-level benchmarking showed that different evidence layers optimize different objectives: effect-based ranking was strongest for held-out replication, whereas pathway and hub scores more strongly concentrated curated migraine biology. The integrated score should therefore be interpreted as a balanced downstream-selection score rather than as a universally dominant ranking. Third, contextual comparison with Open Targets suggests that G2DR is complementary to established evidence-integration platforms: it broadens the exploratory target space and recovers additional migraine-reference genes outside the Open Targets migraine list, while remaining less concentrated within established disease-target space.

The drug-level results are most informative when interpreted through the tiered benchmark rather than the global-background enrichment alone. While the framework recovered migraine-linked compounds above random expectation, recovery was strongest for broader literature-linked, off-label, and shared-mechanism therapeutic space, whereas migraine-specific approved therapies were under-represented in the top-ranked set. This suggests that the current implementation is better at expanding genetics-anchored translational hypothesis space than at reproducing the most indication-specific modern pharmacology. Directionality filtering further strengthened this interpretation by showing that only a subset of recovered compounds retained clear mechanistic compatibility with the inferred disease-associated gene direction. Together, these findings argue that the strongest present use case for G2DR is structured target and drug-hypothesis prioritization rather than direct inference of therapeutic efficacy.

The causal-support analyses are important precisely because they limit overinterpretation. Single-instrument Mendelian randomization yielded nominal associations only in broader ranked sets, no gene survived multiple-testing correction, and colocalization identified no gene-locus pairs with strong shared-signal support. These findings do not negate the prioritization signal, but they do indicate that the current framework is operating at the level of genetics-anchored candidate ranking rather than causal effector-gene identification. In practical terms, G2DR should therefore be viewed as a hypothesis-prioritization framework whose outputs require orthogonal validation, not as a causal target-discovery engine.

Across cross-validation folds, exact overlap among top-ranked genes was limited, which is expected in a modest, class-imbalanced cohort in which each fold contains only a small number of cases. More importantly, prioritization performance was stable at the signal level, and drug-level rankings were substantially more stable than gene-level identities. This distinction is central to interpreting the framework correctly: for a prioritization method, reproducibility of ranking behavior is more informative than perfect recurrence of specific gene lists. The results therefore support stability of the prioritization signal even when individual top-ranked genes vary across folds.

The study has several important limitations. The migraine cohort is modest and class-imbalanced, which constrains power and likely contributes to both instability in individual gene identities and diffuse significance across highly layered testing structures. The framework relies on genetically predicted rather than measured context-specific transcription, and TWAS-style signal remains vulnerable to linkage disequilibrium and co-regulation. Drug mapping is further constrained by database coverage, evidence heterogeneity, and imperfect action-direction annotation. These limitations mean that prioritized genes should be interpreted as genetically supported candidates rather than confirmed causal effectors, and prioritized compounds should be interpreted as computational hypotheses rather than translational recommendations.

Equally informative is what the framework does not yet recover well. The under-representation of serotonergic and CGRP-axis therapies suggests that current public drug-target resources and genetically prioritized gene programs more readily capture shared neurobiological and comorbidity-linked pharmacology than highly indication-specific migraine therapeutics. This operating profile helps explain why broader mechanism-linked candidates are enriched even when migraine-specific approved therapies are sparse in the top-ranked set. Future extensions should therefore focus on stronger causal filters, more explicit perturbational and mechanism-of-action resources, and disease-specific pharmacological annotations that may improve both target specificity and directionality-aware drug ranking.

Overall, G2DR provides a useful foundation for genetics-informed prioritization in genotype-first settings. Its modular design allows independent refinement of transcriptome imputation, gene-level ranking, biological contextualization, and drug mapping, and its present value lies in providing a transparent framework for moving from diffuse inherited signal to a more tractable set of experimentally testable hypotheses. The next critical step is not simply to scale the pipeline, but to strengthen causal attribution, benchmark it more directly against alternative genetics-to-drug workflows, and improve translational specificity through external validation and richer pharmacological annotation. Framed in this way, G2DR is a proof-of-concept prioritization framework with clear room for maturation rather than a finished repurposing engine.

Key Points

- G2DR is a genotype-first computational prioritization framework for hypothesis generation in settings where matched disease transcriptomics are unavailable; it is intended to narrow the space for downstream experimental and translational follow-up rather than to provide clinically actionable target recommendations directly.

- The framework integrates genetically predicted gene expression across seven transcriptome-weight resources, multi-method gene-level testing, pathway enrichment, network context, druggability, and multi-source drug-target evidence into a modular and reproducible prioritization pipeline.
- In held-out internal evaluation, discovery-based gene prioritization generalized to test data (ROC-AUC = 0.775; PR-AUC = 0.475), while the integrated score provided a balanced operating point for downstream target selection rather than maximizing any single benchmark criterion.
- Drug mapping recovered migraine-linked compounds relative to a global background, but the strongest signal lay in broader mechanism-linked and off-label therapeutic space rather than migraine-specific approved therapies; directionality filtering helped distinguish mechanistically coherent hypotheses from broadly associated candidates.
- All prioritized genes and compounds remain computational hypotheses requiring independent pharmacological, mechanistic, and clinical validation; in its current form, G2DR is best viewed as a proof-of-concept framework for genetics-anchored prioritization with clear directions for improvement in causal attribution and translational specificity.

Competing interests

The authors declare no competing interests.

Author contributions statement

M.M. conceived the study, designed and implemented the G2DR framework, performed all analyses, and drafted the manuscript. D.B.A. supervised the project, contributed to study design and interpretation, and reviewed and edited the manuscript. All authors approved the final manuscript.

Funding

This work was supported by the University of Queensland and the Baker Heart and Diabetes Institute. The UK Biobank data were accessed under application ID 50000. The funding sources had no role in study design, data collection, analysis, interpretation, or the decision to submit for publication.

Data and Software Availability

The genotype and phenotype data used in this study were accessed through the UK Biobank under application ID 50000 (<https://www.ukbiobank.ac.uk/>) and are subject to UK Biobank access restrictions; researchers may apply for access through the UK Biobank Access Management System. The G2DR framework source code is freely available for non-commercial use at <https://github.com/MuhammadMuneeb007/G2DR-A-Genotype-First-Framework-for-Genetics-Informed-Target-Prioritization-and-Drug-Repurposing>. Supporting utilities are available at the following repositories: gene phenotype downloader, PhenotypeToGeneDownloaderR (<https://github.com/MuhammadMuneeb007/PhenotypeToGeneDownloaderR>); gene identifier converter, GeneMapKit (<https://github.com/MuhammadMuneeb007/GeneMapKit>); drug-disease downloader, DownloadDrugsRelatedToDiseases (<https://github.com/MuhammadMuneeb007/DownloadDrugsRelatedToDiseases>). All repositories will be maintained for a minimum of two years following publication. Public annotation resources used by the pipeline include STRING (<https://string-db.org>), Open Targets (<https://www.opentargets.org>), DGIdb (<https://www.dgldb.org>), and ChEMBL (<https://www.ebi.ac.uk/chembl>).

Acknowledgments

Not applicable

Author Biographies

Muhammad Muneeb is a PhD candidate at the University of Queensland and Baker Heart and Diabetes Institute, specializing in computational biology.

David B. Ascher is a Professor at the University of Queensland and Baker Heart and Diabetes Institute, leading research in computational structural biology, molecular pharmacology, and translational bioinformatics for drug discovery and precision medicine.

References

1. Ted T. Ashburn and Karl B. Thor. Drug repositioning: identifying and developing new uses for existing drugs. *Nature Reviews Drug Discovery*, 3(8):673–683, August 2004.
2. Sudeep Pushpakom, Francesco Iorio, Patrick A. Eyers, Kieron J. Escott, Shirley Hopper, Andrew Wells, Andrew Doig, Tim Williams, Joanna Latimer, Catherine McNamee, Alison Norris, Philippe Sanseau, Daniela Cavalla, and Munir Pirmohamed. Drug repurposing: progress, challenges and recommendations. *Nature Reviews Drug Discovery*, 18(1):41–58, 2019.
3. Nicola Nosengo. Can you teach old drugs new tricks? *Nature*, 534:314–316, 2016.
4. Justin Lamb, Emily D. Crawford, David Peck, Joshua W. Modell, Irene C. Blat, Matthew J. Wrobel, Jim Lerner, Jean-Philippe Brunet, Aravind Subramanian, Kenneth N. Ross, Michael Reich, Haley Hieronymus, Guo Wei, Scott A. Armstrong, Stephen J. Haggarty, Paul A. Clemons, Ru Wei, Steven A. Carr, Eric S. Lander, and Todd R. Golub. The connectivity map: using gene-expression signatures to connect small molecules, genes, and disease. *Science*, 313(5795):1929–1935, 2006.
5. Andrew L Hopkins. Network pharmacology: the next paradigm in drug discovery. *Nature Chemical Biology*, 4(11):682–690, 2008.
6. Albert-László Barabási, Natali Gulbahce, and Joseph Loscalzo. Network medicine: a network-based approach to human disease. *Nature Reviews Genetics*, 12(1):56–68, 2011.
7. Víctor Martínez and et al. Drugnet: network-based drug-disease prioritization. *Bioinformatics*, 2015.
8. Daniel S. Himmelstein, Antoine Lizee, Christine Hessler, Leo Brueggeman, Sabrina L. Chen, Dexter Hadley, Ari Green, Pouya Khankhanian, and Sergio E. Baranzini. Systematic integration of biomedical knowledge prioritizes drugs for repurposing. *eLife*, 6:e26726, 2017.
9. Marinka Zitnik, Monica Agrawal, and Jure Leskovec. Modeling polypharmacy side effects with graph convolutional networks. *Bioinformatics*, 34(13):i457–i466, 2018.
10. Aravind Subramanian, Rohith Narayan, Steven M. Corsello, David D. Peck, Theodore E. Natoli, Xiaodong Lu, Joshua Gould, John F. Davis, Alberto A. Tubelli, Joseph K. Asiedu, David L. Lahr, Joseph E. Hirschman, Zihan Liu, Michael Donahue, Brian Julian, Mehrtash Khan, David Wadden, Ian C. Smith, Daniel Lam, Arthur Liberzon, Craig Toder, Megan Bagul, Marcin Orzechowski, Oana M. Enache, Francesco Piccioni, Scott A. Johnson, Nicholas J. Lyons, Adam H. Berger, Alykhan F. Shamji, Aaron N. Brooks, Anita Vrcic, Colleen Flynn, Jenna Rosains, Daisuke Y. Takeda, Rong Hu, Daniel Davison, Justin Lamb, Kristin Ardlie, Larson Hogstrom, Peyton Greenside, Nathanael S. Gray, Paul A. Clemons, Seth Silver, Xiaoyun Wu, W. Nicholas Zhao, William Read-Button, Xiao Wu, Stephen J. Haggarty, Luigi V. Ronco, Jesse S. Boehm, Stuart L. Schreiber, John G. Doench, Joshua A. Bittker, David E. Root, Bang Wong, and Todd R. Golub. A next generation connectivity map: L1000 platform and the first 1,000,000 profiles. *Cell*, 171(6):1437–1452.e17, 2017.
11. Amar Koleti, R Terryn, V Stathias, et al. Data portal for the library of integrated network-based cellular signatures (lincs) program. *Nucleic Acids Research*, 46(D1):D558–D566, 2018.
12. Jörg Menche, Amitabh Sharma, Maksim Kitsak, Susan D. Ghassian, Marc Vidal, Joseph Loscalzo, and Albert-László

- Barabási. Uncovering disease–disease relationships through the incomplete interactome. *Science*, 347(6224):1257601, 2015.
13. Cathie Sudlow, John Gallacher, Naomi Allen, Valerie Beral, Paul Burton, John Danesh, Paul Downey, Paul Elliott, Jane Green, Martin Landray, Bette Liu, Paul Matthews, Gideon Ong, Jill Pell, Alan Silman, Alan Young, Tim Sprosen, Tim Peakman, and Rory Collins. UK Biobank: an open access resource for identifying the causes of a wide range of complex diseases of middle and old age. *PLOS Medicine*, 12(3):e1001779, 2015.
 14. Clare Bycroft, Colin Freeman, Desislava Petkova, Gavin Band, Lloyd T. Elliott, Kevin Sharp, Allan Motyer, Damjan Vukcevic, Olivier Delaneau, Jared O’Connell, Adrian Cortes, Samantha Welsh, Gil McVean, Stephen Leslie, Peter Donnelly, and Jonathan Marchini. The UK Biobank resource with deep phenotyping and genomic data. *Nature*, 562(7726):203–209, 2018.
 15. Michael Wainberg, Nasa Sinnott-Armstrong, Nicolo Mancuso, Alvaro N. Barbeira, David A. Knowles, David Golan, Rachel Ermel, Arno Ruusalepp, Thomas Quertermous, Ke Hao, Johan L.M. Björkegren, Hong-Hee Im, Bogdan Pasaniuc, and Manuel A. Rivas. Opportunities and challenges for transcriptome-wide association studies. *Nature Genetics*, 51(4):592–599, 2019.
 16. Eric R. Gamazon, Heather E. Wheeler, Kaan P. Shah, Somayeh V. Mozaffari, Karolina Aquino-Michaels, Rory J. Carroll, Anne E. Eyster, Joshua C. Denny, Dan L. Nicolae, Nancy J. Cox, and Hong-Hee Im. A gene-based association method for mapping traits using reference transcriptome data. *Nature Genetics*, 47(9):1091–1098, 2015.
 17. Alexander Gusev, Arthur Ko, Huwenbo Shi, Gaurav Bhatia, Wendy Chung, Brenda WJH Penninx, Rick Jansen, Eco JC De Geus, Dorret I Boomsma, Fred A Wright, et al. Integrative approaches for large-scale transcriptome-wide association studies. *Nature genetics*, 48(3):245–252, 2016.
 18. Alvaro N. Barbeira, Scott P. Dickinson, Rodrigo Bonazzola, Jiamao Zheng, Heather E. Wheeler, Jason M. Torres, Eric S. Torstenson, Kaanan P. Shah, Tzintzuni Garcia, Todd L. Edwards, Eli A. Stahl, Laura M. Huckins, François Aguet, Kristin G. Ardlie, Beryl B. Cummings, Ellen T. Gelfand, Gad Getz, Kane Hadley, Robert E. Handsaker, Katherine H. Huang, Seva Kashin, Konrad J. Karczewski, Monkol Lek, Xiao Li, Daniel G. MacArthur, Jared L. Nedzel, Duyen T. Nguyen, Michael S. Noble, Ayellet V. Segrè, Casandra A. Trowbridge, Taru Tukiainen, Nathan S. Abell, Brunilda Balliu, Ruth Barshir, Omer Basha, Alexis Battle, Gireesh K. Bogu, Andrew Brown, Christopher D. Brown, Stephane E. Castel, Lin S. Chen, Colby Chiang, Donald F. Conrad, Farhan N. Damani, Joe R. Davis, Olivier Delaneau, Emmanouil T. Dermitzakis, Barbara E. Engelhardt, Eleazar Eskin, Pedro G. Ferreira, Laure Frésard, Eric R. Gamazon, Diego Garrido-Martín, Ariel D. H. Gwartz, Genna Gliner, Michael J. Gludemans, Roderic Guigo, Ira M. Hall, Buhm Han, Yuan He, Farhad Hormozdiari, Cedric Howald, Brian Jo, Eun Yong Kang, Yungil Kim, Sarah Kim-Hellmuth, Tuuli Lappalainen, Gen Li, Xin Li, Boxiang Liu, Serghei Mangul, Mark I. McCarthy, Ian C. McDowell, Pejman Mohammadi, Jean Monlong, Stephen B. Montgomery, Manuel Muñoz-Aguirre, Anne W. Ndungu, Andrew B. Nobel, Meritxell Oliva, Halit Ongen, John J. Palowitch, Nikolaos Panousis, Panagiotis Papasaiakas, YoSon Park, Princy Parsana, Anthony J. Payne, Christine B. Peterson, Jie Quan, Ferran Reverter, Chiara Sabatti, Ashis Saha, Michael Sammeth, Alexandra J. Scott, Andrey A. Shabalin, Reza Sodaei, Matthew Stephens, Barbara E. Stranger, Benjamin J. Strober, Jae Hoon Sul, Emily K. Tsang, Sarah Urbut, Martijn van de Bunt, Gao Wang, Xiaoquan Wen, Fred A. Wright, Hualin S. Xi, Esti Yeger-Lotem, Zachary Zappala, Judith B. Zaugg, Yi-Hui Zhou, Joshua M. Akey, Daniel Bates, Joanne Chan, Lin S. Chen, Melina Claussnitzer, Kathryn Demanelis, Morgan Diegel, Jennifer A. Doherty, Andrew P. Feinberg, Marian S. Fernando, Jessica Halow, Kasper D. Hansen, Eric Haugen, Peter F. Hickey, Lei Hou, Farzana Jasmine, Ruiqi Jian, Lihua Jiang, Audra Johnson, Rajinder Kaul, Manolis Kellis, Muhammad G. Kibriya, Kristen Lee, Jin Billy Li, Qin Li, Xiao Li, Jessica Lin, Shin Lin, Sandra Linder, Caroline Linke, Yaping Liu, Matthew T. Maurano, Benoit Molinie, Stephen B. Montgomery, Jemma Nelson, Fidencio J. Neri, Meritxell Oliva, Yongjin Park, Brandon L. Pierce, Nicola J. Rinaldi, Lindsay F. Rizzardi, Richard Sandstrom, Andrew Skol, Kevin S. Smith, Michael P. Snyder, John Stamatoyannopoulos, Barbara E. Stranger, Hua Tang, Emily K. Tsang, Li Wang, Meng Wang, Nicholas Van Wittenberghe, Fan Wu, Rui Zhang, Concepcion R. Nierras, Philip A. Branton, Latarsha J. Carithers, Ping Guan, Helen M. Moore, Abhi Rao, Jimmie B. Vaught, Sarah E. Gould, Nicole C. Lockart, Casey Martin, Jeffery P. Struewing, Simona Volpi, Anjene M. Addington, Susan E. Koester, A. Roger Little, Lori E. Brigham, Richard Hasz, Marcus Hunter, Christopher Johns, Mark Johnson, Gene Kopen, William F. Leinweber, John T. Lonsdale, Alisa McDonald, Bernadette Mestichelli, Kevin Myer, Brian Roe, Michael Salvatore, Saboor Shad, Jeffrey A. Thomas, Gary Walters, Michael Washington, Joseph Wheeler, Jason Bridge, Barbara A. Foster, Bryan M. Gillard, Ellen Karasik, Rachna Kumar, Mark Miklos, Michael T. Moser, Scott D. Jewell, Robert G. Montroy, Daniel C. Rohrer, Dana R. Valley, David A. Davis, Deborah C. Mash, Anita H. Undale, Anna M. Smith, David E. Tabor, Nancy V. Roche, Jeffrey A. McLean, Negin Vatanian, Karna L. Robinson, Leslie Sobin, Mary E. Barcus, Kimberly M. Valentino, Liqun Qi, Steven Hunter, Pushpa Hariharan, Shilpi Singh, Ki Sung Um, Takunda Matose, Maria M. Tomaszewski, Laura K. Barker, Maghboeba Mosavel, Laura A. Siminoff, Heather M. Traino, Paul Flicek, Thomas Juettemann, Magali Ruffier, Dan Sheppard, Kieron Taylor, Stephen J. Trevanion, Daniel R. Zerbino, Brian Craft, Mary Goldman, Maximilian Haeussler, W. James Kent, Christopher M. Lee, Benedict Paten, Kate R. Rosenbloom, John Vivian, Jingchun Zhu, Dan L. Nicolae, Nancy J. Cox, and Hae Kyung Im. Exploring the phenotypic consequences of tissue specific gene expression variation inferred from gwas summary statistics. *Nature Communications*, 9(1), May 2018.
 19. Matthew R. Nelson, Harriet Tipney, Jeffrey L. Painter, Jessica Shen, Paolo Nicoletti, Yufeng Shen, Aris Floratos, Pak C. Sham, Michael J. Li, Jing Wang, et al. The support of human genetic evidence for approved drug indications. *Nature Genetics*, 47(8):856–860, 2015.
 20. Emily A. King, Jimmy W. Davis, and Jacob F. Degner. Are drug targets with genetic support twice as likely to be approved? revised estimates of the impact of genetic support for drug mechanisms on the probability of drug approval. *PLOS Genetics*, 15(12):e1008489, 2019.

21. David Ochoa, Andrew Hercules, Miguel Carmona, et al. The open targets platform: supporting systematic drug-target identification and prioritisation. *Nucleic Acids Research*, 49(D1):D1302–D1310, 2021.
22. Summer L Freshour, Savannah Kiwala, Kelsy C Cotto, et al. Integration of the drug-gene interaction database (dgidb 4.0). *Nucleic Acids Research*, 49(D1):D1144–D1151, 2021.
23. A. Gaulton, L. J. Bellis, A. P. Bento, J. Chambers, M. Davies, A. Hersey, Y. Light, S. McGlinchey, D. Michalovich, B. Al-Lazikani, and J. P. Overington. ChEMBL: a large-scale bioactivity database for drug discovery. *Nucleic Acids Research*, 40(D1):D1100–D1107, September 2011.
24. Anna Gaulton, Anne Hersey, Michał Nowotka, A. Patrícia Bento, Jon Chambers, David Mendez, Prudence Mutowo, Francis Atkinson, Louisa J. Bellis, Elena Cibrián-Uhalte, Mark Davies, Nathan Dedman, Anneli Karlsson, María Paula Magariños, John P. Overington, George Papadatos, Ines Smit, and Andrew R. Leach. The ChEMBL database in 2017. *Nucleic Acids Research*, 45(D1):D945–D954, November 2016.
25. David S Wishart, Yannick D Feunang, An C Guo, et al. DrugBank 5.0: a major update to the DrugBank database. *Nucleic Acids Research*, 46(D1):D1074–D1082, 2018.
26. Daniel S Araujo, Chris Nguyen, Xiaowei Hu, Anna V Mikhaylova, Christopher Gignoux, Kristin Ardlie, Kent D Taylor, Peter Durda, Yongmei Liu, George Papanicolaou, et al. Multivariate adaptive shrinkage improves cross-population transcriptome prediction and association studies in underrepresented populations. *HGG advances*, 4(4):100250, 2023.
27. Dan Zhou, Yi Jiang, Xiaohong Zhong, Nancy J Cox, Chunyu Liu, and Eric R Gamazon. A unified framework for joint-tissue transcriptome-wide association and mendelian randomization analysis. *Nature genetics*, 52(11):1234–1242, 2020.
28. Yiming Hu, Mo Li, Qiongshi Lu, Haoyi Weng, Jiawei Wang, Seyedeh M. Zekavat, Zhaolong Yu, Boyang Li, Jianlei Gu, Sydney Muchnik, Yu Shi, Brian W. Kunkle, Shubhabrata Mukherjee, Pradeep Natarajan, Adam Naj, Amanda Kuzma, Yi Zhao, Paul K. Crane, Hui Lu, and Hongyu Zhao. A statistical framework for cross-tissue transcriptome-wide association analysis. *Nature Genetics*, 51(3):568–576, February 2019.
29. Wen Zhang, Georgios Voloudakis, Veera M Rajagopal, Ben Readhead, Joel T Dudley, Eric E Schadt, Johan L M Björkegren, Yungil Kim, John F Fullard, Gabriel E Hoffman, et al. Integrative transcriptome imputation reveals tissue-specific and shared biological mechanisms mediating susceptibility to complex traits. *Nature communications*, 10(1):3834, 2019.
30. Sini Nagpal, Xing Meng, Michael P Epstein, Lam C Tsoi, Matthew Patrick, Greg Gibson, Philip L De Jager, David A Bennett, Thomas S Wingo, Aliza P Wingo, et al. TIGER: an improved Bayesian tool for transcriptomic data imputation enhances gene mapping of complex traits. *The American Journal of Human Genetics*, 105(2):258–266, 2019.
31. Dawn C Buse, Adam Manack, Daniel Serrano, Connie Turkel, and Richard B Lipton. Migraine-related disability, impact, and health-related quality of life. *Neurology*, 80(24):2194–2203, 2013.
32. Marcelo E. Bigal and Richard B. Lipton. Migraine and cardiovascular disease: a population-based study. *Neurology*, 72(21):1864–1871, 2009.
33. Parisa Gazerani. Migraine and gastrointestinal disorders: a systematic review. *The Journal of Headache and Pain*, 16:39, 2015.
34. Zaza Katsarava, Dawn C. Buse, Adam N. Manack, and Richard B. Lipton. Migraine and comorbidities. *The Journal of Headache and Pain*, 19(1):126, 2018.
35. Shaun Purcell, Benjamin Neale, Kathryn Todd-Brown, Lori Thomas, Manuel AR Ferreira, David Bender, Julian Maller, Pamela Sklar, Paul IW de Bakker, Mark J Daly, and Pak C Sham. PLINK: a tool set for whole-genome association and population-based linkage analyses. *American Journal of Human Genetics*, 81(3):559–575, 2007.
36. Carl A Anderson, Fredrik H Pettersson, Gerald M Clarke, Lon R Cardon, Andrew P Morris, and Krina T Zondervan. Data quality control in genetic case-control association studies. *Nature Protocols*, 5(9):1564–1573, 2010.
37. Matthew E Ritchie, Belinda Phipson, Di Wu, et al. limma powers differential expression analyses for RNA-sequencing and microarray studies. *Nucleic Acids Research*, 43(7):e47–e47, 2015.
38. Heidi Hautakangas, Bendik S. Winsvold, Sanni E. Ruotsalainen, Gyda Björnsdóttir, Aster V. E. Harder, Lisette J. A. Kogelman, Laurent F. Thomas, Raymond Noordam, Christian Benner, Padhraig Gormley, Ville Artto, Karina Banasik, Anna Björnsdóttir, Dorret I. Boomsma, Ben M. Brumpton, Kristoffer Sølvesten Burgdorf, Julie E. Buring, Mona Ameri Chalmer, Irene de Boer, Martin Dichgans, Christian Erikstrup, Markus Färkkilä, Maiken Elvestad Garbrielsen, Mohsen Ghanbari, Knut Hagen, Paavo Häppölä, Jouke-Jan Hottenga, Maria G. Hrafnisdóttir, Kristian Hveem, Marianne Bakke Johnsen, Mika Kähönen, Espen S. Kristoffersen, Tobias Kurth, Terho Lehtimäki, Lannie Lighthart, Sigurdur H. Magnusson, Rainer Malik, Ole Birger Pedersen, Nadine Pelzer, Brenda W. J. H. Penninx, Caroline Ran, Paul M. Ridker, Frits R. Rosendaal, Gudrun R. Sigurdardóttir, Anne Heidi Skogholt, Olafur A. Sveinsson, Thorgeir E. Thorgeirsson, Henrik Ullum, Lianne S. Vijfhuizen, Elisabeth Widén, Ko Willems van Dijk, Irene de Boer, Arn M. J. M. van den Maagdenberg, Arpo Aromaa, Andrea Carmine Belin, Tobias Freilinger, M. Arfan Ikram, Marjo-Riitta Järvelin, Olli T. Raitakari, Gisela M. Terwindt, Mikko Kallela, Maija Wessman, Jes Olesen, Daniel I. Chasman, Dale R. Nyholt, Hreinn Stefánsson, Kari Stefánsson, Arn M. J. M. van den Maagdenberg, Thomas Folkmann Hansen, Samuli Ripatti, John-Anker Zwart, Aarno Palotie, and Matti Pirinen. Genome-wide analysis of 102, 084 migraine cases identifies 123 risk loci and subtype-specific risk alleles. *Nature Genetics*, 54(2):152–160, February 2022.
39. Padhraig Gormley, Verneri Anttila, Bendik S Winsvold, Priit Palta, Tonu Esko, Tune H Pers, Kai-How Farh, Ester Cuenca-Leon, Mikko Muona, Nicholas A Furlotte, Tobias Kurth, Andres Ingason, George McMahon, Lannie Lighthart, Gisela M Terwindt, Mikko Kallela, Tobias M Freilinger, Caroline Ran, Scott G Gordon, Anine H Stam, Stacy Steinberg, Guntram Borck, Markku Koiranen, Lydia Quaye, Hieab H H Adams, Terho Lehtimäki, Antti-Pekka Sarin, Juho Wedenoja, David A Hinds, Julie E Buring, Markus Schürks, Paul M Ridker, Maria Gudlaug Hrafnisdóttir, Hreinn Stefánsson, Susan M Ring, Jouke-Jan Hottenga, Brenda W J H Penninx, Markus Färkkilä, Ville Artto, Mari Kaunisto, Salli Vepsäläinen, Rainer Malik, Andrew C Heath, Pamela A F Madden, Nicholas G Martin, Grant W Montgomery, Mitja I Kurki, Mart

- Kals, Reedik Mägi, Kalle Pärn, Eija Hämäläinen, Hailiang Huang, Andrea E Byrnes, Lude Franke, Jie Huang, Evie Stergiakouli, Phil H Lee, Cynthia Sandor, Caleb Webber, Zameel Cader, Bertram Muller-Myhsok, Stefan Schreiber, Thomas Meitinger, Johan G Eriksson, Veikko Salomaa, Kauko Heikkilä, Elizabeth Loehrer, Andre G Uitterlinden, Albert Hofman, Cornelia M van Duijn, Lynn Cherkas, Linda M Pedersen, Audun Stubhaug, Christopher S Nielsen, Minna Männikkö, Evelin Mihailov, Lili Milani, Hartmut Göbel, Ann-Louise Esserlind, Anne Francke Christensen, Thomas Folkmann Hansen, Thomas Werge, Jaakko Kaprio, Arpo J Aromaa, Olli Raitakari, M Arfan Ikram, Tim Spector, Marjo-Riitta Järvelin, Andres Metspalu, Christian Kubisch, David P Strachan, Michel D Ferrari, Andrea C Belin, Martin Dichgans, Maija Wessman, Arn M J M van den Maagdenberg, John-Anker Zwart, Dorret I Boomsma, George Davey Smith, Kari Stefansson, Nicholas Eriksson, Mark J Daly, Benjamin M Neale, Jes Olesen, Daniel I Chasman, Dale R Nyholt, and Aarno Palotie. Meta-analysis of 375, 000 individuals identifies 38 susceptibility loci for migraine. *Nature Genetics*, 48(8):856–866, June 2016.
40. Claudia F. Gasparini, Robert A. Smith, and Lyn R. Griffiths. Genetic insights into migraine and glutamate: a protagonist driving the headache. *Journal of the Neurological Sciences*, 367:258–268, August 2016.
41. Giovanna Crivellaro et al. Specific activation of *glun1-n2b* nmda receptors underlies facilitation of cortical spreading depression in a genetic mouse model of migraine with reduced astrocytic glutamate clearance. *Neurobiology of Disease*, 156:105419, 2021.
42. Elena C. Gross, Marco Lisicki, Dirk Fischer, Peter S. Sándor, and Jean Schoenen. The metabolic face of migraine — from pathophysiology to treatment. *Nature Reviews Neurology*, 15(11):627–643, October 2019.
43. Martina Curto, Luana Lionetto, Andrea Negro, Matilde Capi, Francesco Fazio, Maria Adele Giamberardino, Maurizio Simmaco, Ferdinando Nicoletti, and Paolo Martelletti. Altered kynurenine pathway metabolites in serum of chronic migraine patients. *The Journal of Headache and Pain*, 17(1), April 2016.
44. Hulya Karatas, Sefik Evren Erdener, Yasemin Gursoy-Ozdemir, Sevda Lule, Emine Eren-Koçak, Zümrüt Duygu Sen, and Turgay Dalkara. Spreading depression triggers headache by activating neuronal *panx1* channels. *Science*, 339(6123):1092–1095, March 2013.
45. Qiu He, Xiang Lin, Fengzhi Wang, Jialiang Xu, Zhanxiu Ren, Wei Chen, and Xuesha Xing. Associations of a polymorphism in the intercellular adhesion molecule-1 (*icam1*) gene and *icam1* serum levels with migraine in a chinese han population. *Journal of the Neurological Sciences*, 345(1–2):148–153, October 2014.
46. Aelita Plinta, Peteris Tretjakovs, Simons Svirskis, Inara Logina, Gita Gersone, Antra Jurka, Indra Mikelsone, Leons Blumfelds, Vitolds Mackevics, and Guntis Bahs. Association of body mass index, blood pressure, and interictal serum levels of cytokines in migraine with and without aura. *Journal of Clinical Medicine*, 11(19):5696, September 2022.
47. Kenju Hara, Atsushi Shiga, Toshio Fukutake, Hiroaki Nozaki, Akinori Miyashita, Akio Yokoseki, Hirotoshi Kawata, Akihito Koyama, Kunimasa Arima, Toshiaki Takahashi, Mari Ikeda, Hiroshi Shiota, Masato Tamura, Yutaka Shimoe, Mikio Hirayama, Takayo Arisato, Sohei Yanagawa, Akira Tanaka, Imaharu Nakano, Shu-ichi Ikeda, Yutaka Yoshida, Tadashi Yamamoto, Takeshi Ikeuchi, Ryozo Kuwano, Masatoyo Nishizawa, Shoji Tsuji, and Osamu Onodera. Association of *htra1* mutations and familial ischemic cerebral small-vessel disease. *New England Journal of Medicine*, 360(17):1729–1739, April 2009.
48. Matthew D. Shirley, Hao Tang, Carol J. Gallione, Joseph D. Baugher, Laurence P. Frelin, Bernard Cohen, Paula E. North, Douglas A. Marchuk, Anne M. Comi, and Jonathan Pevsner. Sturge–weber syndrome and port-wine stains caused by somatic mutation in *gnas1*. *New England Journal of Medicine*, 368(21):1971–1979, May 2013.
49. Coen Maas and Thomas Renné. Coagulation factor xii in thrombosis and inflammation. *Blood*, 131(17):1903–1909, April 2018.
50. V. Kirthi, S. Derry, and R. A. Moore. Aspirin with or without an antiemetic for acute migraine headaches in adults. *Cochrane Database of Systematic Reviews*, 2013.
51. Sheena Derry, Roy Rabbie, and R. Andrew Moore. Diclofenac with or without an antiemetic for acute migraine headaches in adults. *Cochrane Database of Systematic Reviews*, 2019(5), April 2013.
52. M. J. Marmura and S. W. Goldberg. Celecoxib for acute migraine: a systematic review. *Headache*, 55(3):387–393, 2015.
53. A. Singh, H. J. Alter, and B. Zaia. Does the addition of dexamethasone to standard therapy for acute migraine headache decrease the incidence of recurrent headache for patients treated in the emergency department? a meta-analysis and systematic review of the literature. *Academic Emergency Medicine*, 15(12):1223–1233, 2008.
54. I. Colman, B. W. Friedman, M. D. Brown, G. D. Innes, E. Grafstein, T. E. Roberts, and B. H. Rowe. Parenteral dexamethasone for acute severe migraine headache: meta-analysis of randomised controlled trials for preventing recurrence. *BMJ*, 336(7657):1359–1361, 2008.
55. Eric S Schwenk, Aaron Walter, Marc C Torjman, Sarah Mukhtar, Harsh T Patel, Bryan Nardone, George Sun, Bhavana Thota, Clinton G Lauritsen, and Stephen D Silberstein. Lidocaine infusions for refractory chronic migraine: a retrospective analysis. *Regional Anesthesia and Pain Medicine*, 47(7):408–413, May 2022.
56. J. L. Pomeroy, M. J. Marmura, S. J. Nahas, and E. R. Viscusi. Ketamine infusions for treatment refractory headache. *Headache*, 57(2):276–282, 2017.
57. Christian Lampl, Jan Versijpt, Faisal Mohammad Amin, Christina I. Deligianni, Raquel Gil-Gouveia, Tanvir Jassal, Antoinette MaassenVanDenBrink, Raffaele Ornello, Jakob Paungartner, Margarita Sanchez-del Rio, Uwe Reuter, Derya Uluduz, Tessa de Vries, Dena Zeraatkar, and Simona Sacco. European headache federation (ehf) critical re-appraisal and meta-analysis of oral drugs in migraine prevention—part 1: amitriptyline. *The Journal of Headache and Pain*, 24(1), April 2023.
58. Charles Semba and Thomas Gadek. Development of lifitegrast: a novel t-cell inhibitor for the treatment of dry eye disease. *Clinical Ophthalmology*, page 1083, June 2016.
59. Gerhard Rammes. Neramexane: a moderate-affinity nmda receptor channel blocker: new prospects and indications. *Expert Review of Clinical Pharmacology*, 2(3):231–238, May 2009.
60. Karolina Podkowa, Kamil Czarnacki, Agnieszka Borończyk, Michał Borończyk, and Justyna Paprocka. The nmda

receptor antagonists memantine and ketamine as anti-migraine agents. *Naunyn-Schmiedeberg's Archives of Pharmacology*, 396(7):1371–1398, March 2023.

61. Simone Braca, Cinzia Valeria Russo, Antonio Stornaiuolo, Gennaro Cretella, Angelo Miele, Caterina Giannini, and Roberto De Simone. Effectiveness and tolerability of liraglutide as add-on treatment in patients with obesity and high-frequency or chronic migraine: A prospective pilot study. *Headache: The Journal of Head and Face Pain*, 65(10):1831–1838, June 2025.

Supplementary Material

G2DR: A Genotype-First Framework for Genetics-Informed Target Prioritization and Drug Repurposing

Muhammad Muneeb^{1,2} and David B. Ascher^{1,2,*}

¹School of Chemistry and Molecular Biology, The University of Queensland, Queen Street, 4067, Queensland, Australia

²Computational Biology and Clinical Informatics, Baker Heart and Diabetes Institute, Commercial Road, 3004, Victoria, Australia

*Corresponding author: David B. Ascher, d.ascher@uq.edu.au

Contents of this Supplementary Material

This document contains four supplementary methods sections and six supplementary tables. The supplementary methods provide complete mathematical details for the genetically predicted gene expression computation, differential expression analysis, gene prioritization scoring, statistical evaluation framework, and directionality annotation criteria that are summarized in the main manuscript. The supplementary tables provide full results for analyses that are referenced by summary statistics in the main text.

- **Supplementary Methods S1.** Full mathematical specification of genetically predicted gene expression computation (Equations 1–2) and all eight differential expression and association methods (Equations 3–4). Referenced in the main text Methods section under Genetically Predicted Gene Expression and Differential Expression Analysis.
- **Supplementary Methods S2.** Full scoring formulas for the composite importance score (S_g), including reproducibility (R_g), effect magnitude (E_g), statistical confidence (C_g), PathwayScore propagation, and integrated CoreScore computation. Referenced in the main text Methods section under Gene Prioritization.

- **Supplementary Methods S3.** Full derivation of the hypergeometric enrichment test, permutation-based ranking significance test, and fold-enrichment formula used throughout the Results section. Referenced in the main text Methods section under Gene Prioritization.
 - **Supplementary Methods S4.** Full directionality annotation criteria, action vocabulary, and classification rules for gene–drug pair directionality assessment. Referenced in the main text Methods section under Directionality Assessment.
 - **Supplementary Table S1.** Weight stability analysis of the integrated scoring framework across 17 alternative weighting schemes. Referenced in the main text at the Unified Gene Prioritization Framework section.
 - **Supplementary Table S2.** Sensitivity analysis of gene prioritization under stricter FDR and effect-size significance thresholds. Referenced in the main text at the Gene Prioritization Robustness section.
 - **Supplementary Table S3.** Discovery disease-enrichment for curated migraine genes across all expression-weight databases, tissues, and analytical methods. Referenced in the main text at the Component-Based Recovery section.
 - **Supplementary Table S4.** Full comparison of individual evidence components and composite scores across two evaluation universes. Referenced in the main text at the Unified Gene Prioritization Framework section.
 - **Supplementary Table S5.** Multi- K overlap evaluation of predicted drugs against the curated migraine reference drug set for top- N input genes ($N = 200$ and $N = 500$) under two evaluation universes. Referenced in the main text at the Drug Mapping and Candidate Enrichment section.
 - **Supplementary Table S6.** External contextual comparison of G2DR with the Open Targets migraine disease-target resource for migraine gene recovery. Referenced in the main text at the Significant Gene Comparison Against Open Targets section.
-

Supplementary Methods S1. Genetically Predicted Gene Expression and Differential Expression Analysis

Expression prediction. For individual i , gene g , and tissue t , genetically predicted expression was computed as a weighted linear combination of SNP dosages:

$$\widehat{E}_{i,g,t} = \alpha_{g,t} + \sum_{j \in S_g} G_{ij} w_{j,g,t}, \quad (1)$$

where $G_{ij} \in [0, 2]$ is the allelic dosage of SNP j for individual i , $w_{j,g,t}$ is the pre-trained SNP weight for gene g in tissue t , S_g is the set of SNPs used by the model, and $\alpha_{g,t}$ is an intercept term. Covariate-adjusted predicted expression was obtained by regressing out sex and the top 10 genetic principal components estimated from the training split:

$$\widehat{E}_{i,g,t}^{\text{adj}} = \widehat{E}_{i,g,t} - \left(\widehat{\gamma}_{g,t} + \widehat{\delta}_{g,t} \text{Sex}_i + \sum_{k=1}^{10} \widehat{\beta}_{k,g,t} \text{PC}_{ik} \right) + \overline{\widehat{E}}_{g,t}, \quad (2)$$

where $\widehat{\gamma}_{g,t}$, $\widehat{\delta}_{g,t}$, and $\widehat{\beta}_{k,g,t}$ were estimated by ordinary least squares on the training split and applied to validation and test splits without refitting. $\overline{\widehat{E}}_{g,t}$ denotes the training-split mean of $\widehat{E}_{i,g,t}$.

Differential expression methods. For each gene g and tissue t , the case-control mean difference was computed as:

$$\mu_{g,t}^{(1)} = \frac{1}{n_1} \sum_{i:y_i=1} \widehat{E}_{i,g,t}^{\text{adj}}, \quad \mu_{g,t}^{(0)} = \frac{1}{n_0} \sum_{i:y_i=0} \widehat{E}_{i,g,t}^{\text{adj}}, \quad \Delta_{g,t} = \mu_{g,t}^{(1)} - \mu_{g,t}^{(0)}. \quad (3)$$

Five differential-expression methods were applied: (i) LIMMA empirical Bayes moderated t -test with effect estimate taken as the fitted phenotype coefficient; (ii) Welch’s unequal-variance t -test with effect estimate equal to the mean difference; (iii) OLS regression of expression on phenotype y_i with effect estimate taken as the regression coefficient; (iv) Wilcoxon rank-sum test with effect estimate defined as the median difference; and (v) phenotype-label permutation test using $B = 1,000$ random permutations of y_i with an empirical two-sided p -value computed from the permutation distribution of label-shuffled mean differences. Three association-style models treated disease status as the outcome and expression as the predictor. Adjusted expression was standardized to $z_{i,g,t}$ and a logistic model was fitted:

$$\Pr(y_i = 1 \mid z_{i,g,t}) = \frac{1}{1 + \exp[-(\theta_{0,g,t} + \theta_{1,g,t} z_{i,g,t})]}, \quad (4)$$

using weighted logistic regression, bias-reduced Firth logistic regression, and a Bayesian

logistic approximation. Gene-wise nominal p -values were adjusted using the Benjamini–Hochberg procedure, yielding $\text{FDR}_{g,t}^{(m)}$. Genes were considered significant if $\text{FDR}_{g,t}^{(m)} < 0.1$ and $|\log_2 \text{FC}| \geq 0.5$ for differential-expression methods, or $|\text{Effect}| \geq 0.5$ for association-style methods.

Supplementary Methods S2. Gene Prioritization Scoring

Composite importance score. For each candidate gene $g \in G_{\text{discovery}}$, the composite importance score is $S_g = 0.4 R_g + 0.3 E_g + 0.3 C_g$. Reproducibility was quantified as $R_g = 0.6 \text{norm_hits}_g + 0.4 \text{norm_breadth}_g$, where norm_hits_g is the total number of significant occurrences of g across all databases, tissues, methods, and folds normalized to $[0, 1]$ by dividing by the empirical maximum, and norm_breadth_g is the number of unique database–tissue–method combinations in which g was significant, similarly normalized. Effect magnitude was computed by standardizing $|\widehat{\psi}_{g,t}^{(m)}|$ within each method m , then aggregating to the gene level as $E_g = 0.7 f(\bar{e}_g) + 0.3 f(e_g^{\max})$, where $f(\cdot)$ is a smooth monotonic mapping to $[0, 1]$, \bar{e}_g is the mean standardized absolute effect, and e_g^{\max} is the maximum; if all non-zero effect directions for g were consistent in sign, E_g was multiplied by 1.1 to reward directional stability. Statistical confidence was computed as $C_g = 0.6 (1 - \text{FDR}_g^{\min}) + 0.4 (1 - \overline{\text{FDR}}_g)$, where FDR_g^{\min} is the minimum FDR across all significant results and $\overline{\text{FDR}}_g$ is the mean FDR. Reproducibility was weighted highest (40%) because cross-model replication reduces method-specific artefacts, consistent with TWAS prioritization guidance and the winner’s curse literature; effect magnitude and statistical confidence were weighted equally (30% each) to balance biological relevance with statistical support.

PathwayScore propagation. Enrichment was performed using `clusterProfiler::enrichGO`, `clusterProfiler::enrichKEGG`, `ReactomePA::enrichPathway`, and `DOSE::enrichDO` on top- K foreground sets ($K \in \{50, 100, 200, 500, 1000, 2000\}$) with the full tested universe U as background. For each significant enriched term t , a weight was assigned as $\text{weight}(t) = \text{strength}(t) \times \text{robustness}(t)$, where $\text{strength}(t) = -\log_{10}(\text{FDR}_t)$ and $\text{robustness}(t) = n_{\text{hits}}(t)$ counts recurrence of term t as significant across multiple K thresholds and enrichment databases. The PathwayScore for gene g was then $\text{PathwayScore}(g) = \sum_{t: g \in \text{Genes}(t)} \text{weight}(t)$, with genes absent from all enriched-term overlap lists assigned $\text{PathwayScore}(g) = 0$.

Integrated CoreScore. The final integrated score combines four evidence layers as a weighted sum: $\text{CoreScore}_g = 0.45 \cdot \text{DE}_g^{\text{norm}} + 0.25 \cdot \text{Path}_g^{\text{norm}} + 0.25 \cdot \text{Drug}_g^{\text{norm}} + 0.05 \cdot \text{Hub}_g^{\text{norm}}$, where all components were percentile-normalized before combination. Differential expression received the highest weight (0.45) because it provides the primary TWAS-derived genetic link between genotype and disease. Pathway and druggability scores received equal moderate weights (0.25 each) to balance biological coherence with therapeutic tractability. Hub score was down-weighted (0.05) because network centrality often reflects pleiotropy, risking prioritization of non-specific, highly connected genes over disease-specific targets. Hub score was derived from STRING-based degree, betweenness, closeness, and

eigenvector centrality metrics combined into a single network-priority score. Druggability was assessed by querying DGIdb and ChEMBL for known drug interactions (knowledge-based druggability) and applying `fpocket` to PDB or AlphaFold structures for genes without known drug interactions (structure-based druggability).

Supplementary Methods S3. Statistical Evaluation Framework

ROC-AUC and PR-AUC. Generalizability of the composite score was assessed over the full tested universe $U = 34,355$ genes by assigning binary replication labels $y_g = \mathbb{I}(g \in G_{\text{test}})$, where G_{test} comprises genes significant in the held-out test split, and using S_g (or CoreScore _{g}) as the ranking predictor. ROC-AUC and PR-AUC were computed over all genes in U , with genes outside the discovery set assigned a score of zero. The baseline PR-AUC under random ranking equals $T/U = 0.2079$, so the observed PR-AUC of 0.4754 corresponds to a $2.29\times$ lift over random.

Hypergeometric enrichment test. For a top- K list $P_K \subseteq U$ and a positive set of size K^+ (either test-positive genes or curated migraine genes), the hypergeometric p -value is $p_{\text{hyper}} = \Pr(X \geq x)$ for $X \sim \text{Hypergeometric}(N = |U|, K^+, n = |P_K|)$, where $x = |P_K \cap \text{positives}|$ is the observed overlap. Expected overlap under random sampling is $k_{\text{exp}} = |P_K| \times (K^+ / |U|)$, and fold-enrichment is $\text{FE} = k_{\text{obs}} / k_{\text{exp}}$.

Permutation test. Statistical significance of the observed ROC-AUC and PR-AUC was evaluated using 1,000 random permutations of gene scores $\{S_g\}$ while holding labels $\{y_g\}$ fixed, yielding empirical p -values of 9.99×10^{-4} for both metrics (minimum attainable $p = 1/1001$), confirming that the observed ranking lift is not attributable to chance.

Supplementary Methods S4. Directionality Annotation Criteria

Gene direction was assigned from the differential-expression ranking as *higher in cases* (positive mean difference $\Delta_{g,t} > 0$), *lower in cases* (negative mean difference $\Delta_{g,t} < 0$), or *unclear* (conflicting directions across tissues or methods, or no consistent directional signal). Drug action annotations were first extracted from locally aggregated drug–target evidence fields including mechanism-of-action, interaction-type, and directionality fields compiled from Open Targets, DGIdb, and ChEMBL during the drug-mapping step. For pairs lacking explicit local mechanism information, additional annotations were retrieved from ChEMBL by compound identifier and from DGIdb by gene symbol, and were harmonized into a reduced action vocabulary comprising six categories: *inhibitor*, *antagonist*, *agonist*, *activator*, *modulator*, and *unknown*. Each unique gene–drug pair was then classified using the following rules: (i) *directionally consistent* if the drug action was mechanistically compatible with the inferred gene direction — specifically, if the drug is an inhibitor or antagonist against a gene inferred to be higher in cases, or if the drug is an agonist or activator for a gene inferred to be lower in cases; (ii) *directionally inconsistent* if the drug action was opposite to this expectation; and (iii) *unclear* if the gene direction was unresolved, if the drug action was classified as modulator or unknown, or if available annotations were insufficient to support a confident directional interpretation. Directionality was summarized at the level of unique drug–gene pairs to avoid inflation from repeated evidence records for the same pair across multiple databases.

Table S1: Supplementary Table S1. Weight stability analysis of the integrated scoring framework across 17 alternative weighting schemes. Nine reasonable alternative schemes (panel A) and eight extreme single-component stress tests (panel B) were evaluated against the default integrated weights (DE = 0.45, Pathway = 0.25, Drug = 0.25, Hub = 0.05). For each scheme, Spearman ρ against the default ranking, mean Top-100 gene overlap (%), DISC-universe test ROC-AUC (discovery set only, $n = 9,305$ genes), and FULL-universe test ROC-AUC (all $U = 34,355$ tested genes) are reported. Across reasonable alternatives, mean $\rho = 0.963$ (minimum 0.866) and FULL-universe ROC-AUC ranged from 0.775 to 0.776, confirming stability within the biologically justified parameter space. Extreme single-component schemes diverged substantially (mean $\rho = 0.682$; minimum $\rho = 0.292$ for hub-only), confirming that the integrated score draws on genuine multi-source signal.

| Scheme | DE | Path | Drug | Hub | Spearman ρ | Top-100 overlap (%) | DISC ROC-AUC | FULL ROC-AUC |
|--|------|------|------|------|-----------------|---------------------|--------------|--------------|
| (A) Reasonable alternative schemes | | | | | | | | |
| Default (reference) | 0.45 | 0.25 | 0.25 | 0.05 | 1.000 | 100.0 | 0.546 | 0.776 |
| DE-heavy | 0.60 | 0.15 | 0.20 | 0.05 | 0.978 | 84.0 | 0.546 | 0.776 |
| Pathway-heavy | 0.30 | 0.40 | 0.25 | 0.05 | 0.951 | 78.0 | 0.545 | 0.775 |
| Drug-heavy | 0.30 | 0.25 | 0.40 | 0.05 | 0.962 | 82.0 | 0.546 | 0.775 |
| Equal weights (no hub) | 0.33 | 0.33 | 0.33 | 0.00 | 0.941 | 77.0 | 0.545 | 0.775 |
| Equal weights (with hub) | 0.25 | 0.25 | 0.25 | 0.25 | 0.866 | 74.0 | 0.544 | 0.775 |
| No hub | 0.47 | 0.27 | 0.27 | 0.00 | 0.972 | 83.0 | 0.546 | 0.776 |
| DE + pathway only | 0.50 | 0.50 | 0.00 | 0.00 | 0.948 | 78.0 | 0.545 | 0.775 |
| DE + drug only | 0.50 | 0.00 | 0.50 | 0.00 | 0.955 | 80.0 | 0.547 | 0.776 |
| Pathway + drug balanced | 0.40 | 0.30 | 0.30 | 0.00 | 0.963 | 82.0 | 0.546 | 0.776 |
| (B) Extreme single-component stress tests | | | | | | | | |
| DE only | 1.00 | 0.00 | 0.00 | 0.00 | 0.712 | 58.0 | 0.675 | 0.790 |
| Pathway only | 0.00 | 1.00 | 0.00 | 0.00 | 0.651 | 51.0 | 0.529 | 0.549 |
| Drug only | 0.00 | 0.00 | 1.00 | 0.00 | 0.683 | 55.0 | 0.511 | 0.730 |
| Hub only | 0.00 | 0.00 | 0.00 | 1.00 | 0.292 | 32.0 | 0.520 | 0.713 |
| DE + hub only | 0.50 | 0.00 | 0.00 | 0.50 | 0.698 | 56.0 | 0.538 | 0.762 |
| Pathway + hub only | 0.00 | 0.50 | 0.00 | 0.50 | 0.614 | 48.0 | 0.524 | 0.630 |
| Drug + hub only | 0.00 | 0.00 | 0.50 | 0.50 | 0.658 | 52.0 | 0.515 | 0.721 |
| No pathway, no drug | 0.95 | 0.00 | 0.00 | 0.05 | 0.731 | 60.0 | 0.658 | 0.785 |

Table S2: Supplementary Table S2. Sensitivity analysis of gene prioritization under stricter significance thresholds. For each threshold rule, we report the number of significant genes in the training, validation, and held-out test splits; the size of the discovery set ($G_{\text{discovery}}$); held-out ranking performance (ROC-AUC and PR-AUC evaluated over all $U = 34,355$ tested genes); enrichment of discovery genes for held-out test positives (FE test, $T = 7,141$); and enrichment for curated migraine genes (FE migraine, $|M \cap U| = 3,190$). The primary analysis uses $\text{FDR} < 0.10$ and $|\log_2 \text{FC}| \geq 0.50$ (first row). All stricter settings preserved the main prioritization conclusions: held-out ROC-AUC remained above 0.70, fold-enrichment for test positives ranged from 2.58-fold to 3.20-fold, and fold-enrichment for curated migraine genes ranged from 1.38-fold to 1.41-fold. These results indicate that the main gene-prioritization findings are not driven by permissive significance filtering.

| Threshold rule | Train | Validation | Test | $G_{\text{discovery}}$ | ROC-AUC | PR-AUC | FE test | FE migraine |
|---|-------|------------|-------|------------------------|---------|--------|---------|-------------|
| $\text{FDR} < 0.10, \log_2 \text{FC} \geq 0.50$ | 1,046 | 9,107 | 7,141 | 9,305 | 0.7753 | 0.4754 | 2.58 | 1.38 |
| $\text{FDR} < 0.05, \log_2 \text{FC} \geq 0.50$ | 958 | 7,861 | 5,313 | 8,135 | 0.7314 | 0.3412 | 2.62 | 1.39 |
| $\text{FDR} < 0.10, \log_2 \text{FC} \geq 0.75$ | 263 | 6,241 | 4,599 | 6,303 | 0.7339 | 0.3289 | 3.20 | 1.39 |
| $\text{FDR} < 0.05, \log_2 \text{FC} \geq 0.75$ | 248 | 5,709 | 3,772 | 5,794 | 0.7025 | 0.2497 | 3.12 | 1.41 |

Table S3: Supplementary Table S3. Discovery disease-enrichment for curated migraine genes across expression-weight databases, tissues, and analytical methods. For each component, the discovery set comprises unique genes significant at least once in training and validation within that component. Enrichment is computed against curated migraine genes ($M = 3,190$) within the analysis universe (U^*). FE denotes fold-enrichment ($k_{\text{obs}}/k_{\text{exp}}$). Empirical p -values are from size-matched random gene-set sampling ($n_{\text{perm}} = 10,000$).

| Component | N_{pred} | k_{obs} | k_{exp} | FE | p_{emp} |
|---|-------------------|------------------|------------------|------|------------------------|
| (A) Expression-weight databases | | | | | |
| MASHR | 187 | 40 | 17.40 | 2.30 | 1.00×10^{-4} |
| JTI | 104 | 18 | 9.68 | 1.86 | 6.799×10^{-3} |
| FUSION | 9,146 | 1,156 | 851.16 | 1.36 | 1.00×10^{-4} |
| EpiXcan | 34 | 5 | 3.16 | 1.58 | 2.06×10^{-1} |
| CTIMP | 16 | 2 | 1.49 | 1.34 | 4.51×10^{-1} |
| TIGAR | 16 | 2 | 1.49 | 1.34 | 4.48×10^{-1} |
| UTMOST | 3 | 0 | 0.28 | 0.00 | 1.00 |
| (B) Tissues (top 10 by discovery enrichment) | | | | | |
| Brain Amygdala | 312 | 57 | 29.04 | 1.96 | 1.00×10^{-4} |
| Minor Salivary Gland | 315 | 57 | 29.31 | 1.94 | 1.00×10^{-4} |
| Whole Blood | 381 | 65 | 35.46 | 1.83 | 1.00×10^{-4} |
| Adrenal Gland | 399 | 67 | 37.13 | 1.80 | 1.00×10^{-4} |
| Esophagus Gastroesophageal Junction | 419 | 70 | 38.99 | 1.80 | 1.00×10^{-4} |
| Cells EBV-transformed Lymphocytes | 366 | 61 | 34.06 | 1.79 | 1.00×10^{-4} |
| Brain Anterior Cingulate Cortex BA24 | 309 | 51 | 28.76 | 1.77 | 2.00×10^{-4} |
| Brain Spinal Cord Cervical C-1 | 312 | 51 | 29.04 | 1.76 | 1.00×10^{-4} |
| Lung | 502 | 80 | 46.72 | 1.71 | 1.00×10^{-4} |
| Artery Coronary | 380 | 60 | 35.36 | 1.70 | 1.00×10^{-4} |
| (C) Analytical methods | | | | | |
| Weighted Logistic | 9,299 | 1,189 | 865.39 | 1.37 | 1.00×10^{-4} |
| Bayesian Logistic | 9,264 | 1,184 | 862.13 | 1.37 | 1.00×10^{-4} |
| Welch t -test | 917 | 115 | 85.34 | 1.35 | 6.00×10^{-4} |
| Linear Regression | 19 | 2 | 1.77 | 1.13 | 5.36×10^{-1} |
| LIMMA | 19 | 1 | 1.77 | 0.57 | 8.53×10^{-1} |
| Firth Logistic | 3 | 0 | 0.28 | 0.00 | 1.00 |

Table S4: Supplementary Table S4. Comparison of individual evidence components and composite scores across two evaluation universes. Full universe ($U = 34,355$ genes): non-discovery genes receive score = 0; measures pipeline-level separation of discovery-relevant genes from the entire tested space. **Discovery universe ($n = 9,305$ genes): discovery set only (train \cup val); measures within-set ranking quality. T ROC = test-replication ROC-AUC; T PR = test-replication PR-AUC; K ROC = known-migraine ROC-AUC; K PR = known-migraine PR-AUC. Top-200 FE_{test} and FE_{mig} denote fold-enrichment relative to random expectation. Expected Top-200 overlap: full-universe test = 41.57, full-universe migraine = 18.57; disc-universe test = 107.36, disc-universe migraine = 25.56. All raw components were percentile-normalized before ranking.**

| Ranking | AUC metrics | | | | Top-200 test | | Top-200 migraine | |
|--|-------------|-------|-------|-------|--------------|------|------------------|------|
| | T ROC | T PR | K ROC | K PR | Obs | FE | Obs | FE |
| (A) Full universe ($U = 34,355$ genes; non-discovery genes scored as 0) | | | | | | | | |
| Significance only | 0.776 | 0.477 | 0.557 | 0.107 | 146 | 3.51 | 25 | 1.35 |
| Effect only | 0.790 | 0.526 | 0.558 | 0.111 | 145 | 3.49 | 37 | 1.99 |
| Primary composite (S_g) | 0.775 | 0.475 | 0.557 | 0.109 | 156 | 3.75 | 36 | 1.94 |
| Pathway only | 0.549 | 0.265 | 0.520 | 0.108 | 150 | 3.61 | 66 | 3.55 |
| Hub only | 0.713 | 0.396 | 0.572 | 0.135 | 114 | 2.74 | 64 | 3.45 |
| Druggability only | 0.730 | 0.408 | 0.566 | 0.112 | 116 | 2.79 | 25 | 1.35 |
| Direct target evidence only | 0.629 | 0.320 | 0.543 | 0.109 | 110 | 2.65 | 57 | 3.07 |
| Drug-link count only | 0.771 | 0.440 | 0.561 | 0.111 | 105 | 2.53 | 26 | 1.40 |
| Integrated | 0.776 | 0.472 | 0.562 | 0.118 | 140 | 3.37 | 49 | 2.64 |
| (B) Discovery universe ($n = 9,305$ genes; train \cup val only) | | | | | | | | |
| Significance only | 0.548 | 0.593 | 0.505 | 0.131 | 146 | 1.36 | 25 | 0.98 |
| Effect only | 0.675 | 0.663 | 0.519 | 0.140 | 145 | 1.35 | 37 | 1.45 |
| Primary composite (S_g) | 0.543 | 0.590 | 0.510 | 0.135 | 156 | 1.45 | 36 | 1.41 |
| Pathway only | 0.529 | 0.564 | 0.536 | 0.162 | 150 | 1.40 | 66 | 2.58 |
| Hub only | 0.520 | 0.551 | 0.629 | 0.210 | 114 | 1.06 | 64 | 2.50 |
| Druggability only | 0.511 | 0.544 | 0.569 | 0.148 | 121 | 1.13 | 29 | 1.14 |
| Direct target evidence only | 0.511 | 0.543 | 0.542 | 0.152 | 110 | 1.02 | 58 | 2.27 |
| Drug-link count only | 0.505 | 0.539 | 0.553 | 0.141 | 109 | 1.02 | 30 | 1.17 |
| Integrated | 0.546 | 0.585 | 0.562 | 0.161 | 140 | 1.30 | 49 | 1.92 |

Table S5: Supplementary Table S5. Multi- K overlap evaluation of predicted drugs against the curated migraine reference drug set ($|\mathcal{R}| = 4,824$ normalized drugs). Results are shown for top- N input genes ($N = 200$ and $N = 500$) under two evaluation universes. **ALL: global background of 139,597 drugs; hypergeometric enrichment test is valid. **PREDICTED**: returned candidate pool only; FE values below 1.0 reflect the fact that the reference drug set exceeds the returned candidate pool in size, making standard hypergeometric enrichment interpretation inapplicable — AUROC and AUPRC are the appropriate metrics in this frame. Within-set performance: for $N = 200$, AUROC = 0.8004 and AUPRC = 0.3528 (353 curated migraine drugs among 3,963 predicted drugs); for $N = 500$, AUROC = 0.8152 and AUPRC = 0.3311 (527 curated migraine drugs among 7,981 predicted drugs).**

| N | Universe | K | $ \mathcal{U} $ | $ \mathcal{R} $ | Overlap | Prec@K | Rec@K | F1@K | Expected | FE |
|---|-----------|-----|-----------------|-----------------|---------|--------|----------|----------|----------|--------|
| Top-$N = 200$ input genes | | | | | | | | | | |
| 200 | ALL_DRUGS | 20 | 139,597 | 4,824 | 5 | 0.250 | 0.001036 | 0.002064 | 0.691 | 7.235 |
| 200 | ALL_DRUGS | 50 | 139,597 | 4,824 | 20 | 0.400 | 0.004146 | 0.008207 | 1.728 | 11.575 |
| 200 | ALL_DRUGS | 100 | 139,597 | 4,824 | 51 | 0.510 | 0.010572 | 0.020715 | 3.456 | 14.758 |
| 200 | ALL_DRUGS | 200 | 139,597 | 4,824 | 89 | 0.445 | 0.018449 | 0.035430 | 6.911 | 12.877 |
| 200 | ALL_DRUGS | 500 | 139,597 | 4,824 | 205 | 0.410 | 0.042496 | 0.077010 | 17.278 | 11.865 |
| 200 | PREDICTED | 20 | 3,963 | 4,824 | 5 | 0.250 | 0.001036 | 0.002064 | 24.345 | 0.205 |
| 200 | PREDICTED | 50 | 3,963 | 4,824 | 20 | 0.400 | 0.004146 | 0.008207 | 60.863 | 0.329 |
| 200 | PREDICTED | 100 | 3,963 | 4,824 | 51 | 0.510 | 0.010572 | 0.020715 | 121.726 | 0.419 |
| 200 | PREDICTED | 200 | 3,963 | 4,824 | 89 | 0.445 | 0.018449 | 0.035430 | 243.452 | 0.366 |
| 200 | PREDICTED | 500 | 3,963 | 4,824 | 205 | 0.410 | 0.042496 | 0.077010 | 608.630 | 0.337 |
| Top-$N = 500$ input genes | | | | | | | | | | |
| 500 | ALL_DRUGS | 20 | 139,597 | 4,824 | 8 | 0.400 | 0.001658 | 0.003303 | 0.691 | 11.575 |
| 500 | ALL_DRUGS | 50 | 139,597 | 4,824 | 20 | 0.400 | 0.004146 | 0.008207 | 1.728 | 11.575 |
| 500 | ALL_DRUGS | 100 | 139,597 | 4,824 | 53 | 0.530 | 0.010987 | 0.021527 | 3.456 | 15.337 |
| 500 | ALL_DRUGS | 200 | 139,597 | 4,824 | 93 | 0.465 | 0.019279 | 0.037022 | 6.911 | 13.456 |
| 500 | ALL_DRUGS | 500 | 139,597 | 4,824 | 213 | 0.426 | 0.044154 | 0.080015 | 17.278 | 12.328 |
| 500 | PREDICTED | 20 | 7,981 | 4,824 | 8 | 0.400 | 0.001658 | 0.003303 | 12.089 | 0.662 |
| 500 | PREDICTED | 50 | 7,981 | 4,824 | 20 | 0.400 | 0.004146 | 0.008207 | 30.222 | 0.662 |
| 500 | PREDICTED | 100 | 7,981 | 4,824 | 53 | 0.530 | 0.010987 | 0.021527 | 60.444 | 0.877 |
| 500 | PREDICTED | 200 | 7,981 | 4,824 | 93 | 0.465 | 0.019279 | 0.037022 | 120.887 | 0.769 |
| 500 | PREDICTED | 500 | 7,981 | 4,824 | 213 | 0.426 | 0.044154 | 0.080015 | 302.218 | 0.705 |

Table S6: Supplementary Table S6. External contextual comparison of G2DR with the Open Targets migraine disease-target resource for migraine gene recovery. The full G2DR analysis was evaluated across the complete ranked gene universe ($n = 9,305$ genes). The target-filtered G2DR analysis was restricted to genes represented in the Open Targets migraine target space ($n = 823$ genes). Overall recovery is shown against the curated migraine reference set ($M = 3,190$ genes), together with Top- K precision before and after filtering. The substantially higher precision of standalone Open Targets (Top-50: 92.00%) reflects its disease-curated, pre-filtered design rather than a direct performance comparison with G2DR. G2DR operates across a wider gene universe and recovered 725 curated migraine reference genes absent from Open Targets entirely, indicating that the two resources are complementary rather than directly competitive.

| Metric | G2DR (all genes) | G2DR (target-filtered) | Open Targets |
|--|-------------------------|-------------------------------|---------------------|
| Ranked / returned genes | 9,305 | 823 | 2,376 |
| Reference genes recovered | 1,189 | 464 | 1,228 |
| Reference recovery (%) | 37.27 | 14.55 | 38.50 |
| Shared with Open Targets | 823 | 823 | – |
| Shared with Open Targets and reference | 464 | 464 | 464 |
| Reference genes recovered but absent from Open Targets | 725 | 0 | – |
| Top-50 precision (%) | 22.00 | 46.00 | 92.00 |
| Top-100 precision (%) | 22.00 | 50.00 | 95.00 |
| Top-200 precision (%) | 23.00 | 55.50 | 92.50 |
| Top-500 precision (%) | 27.60 | 56.60 | 92.00 |

End of Supplementary Material